

REVIEW ARTICLE

Review of black surfaces for space-borne infrared systems

M. J. Persky^{a)}

Lincoln Laboratory, Massachusetts Institute of Technology, 244 Wood Street, Lexington, Massachusetts 02420-9108

(Received 18 March 1998; accepted for publication 5 January 1999)

Low reflectivity (“black”) surface treatments for space-borne infrared systems are reviewed. The uses of black surfaces in general, as well as for specific space-borne applications are discussed. Compositions of a wide variety of surface treatments with examples of experimental data to characterize performances are provided. Specific treatments included are: Ames 24E paint; AZKO 463 (Sikkens, Cat-A-Lac) paint; Ball IR black paint; Chemglaze (Aeroglaze) Z306 and Z302 paints; Eccosorb 268E paint; Parsons Black paint; black anodize; black Hardlub; black Hardcoat; Martin Black; InfraBlack; Enhanced Martin Black; Ebonal C; Teflon; ion beam textured; appliqués; black chrome; black etched beryllium on beryllium; plasma sprayed boron on beryllium; plasma sprayed beryllium on beryllium; boron carbide on POCO graphite; and Kapton. Data presented for some but not all of the surfaces include: spectrally integrated, 5–25 μm hemispherical-directional reflectance; spectral reflectance at wavelengths between 2 and 500 μm for a variety of incident angles from 5° to 80°; and bidirectional reflectance at a number of wavelengths between 5 and 300 μm for a variety of incident angles from 0° to 80°. The instrumentation employed to obtain these data is briefly described. Long term stability of optical performance, as well as manufacturing reproducibility is demonstrated for several of the surfaces. Outgassing and atomic oxygen interaction information is also included. Methodology for calorimetric measurement of hemispherical emittance as an alternative to optical measurements is given. © 1999 American Institute of Physics.

[S0034-6748(99)00105-7]

I. INTRODUCTION

Low reflectivity¹ (“black”) surfaces have a number of applications for space-borne infrared instruments. Examples are telescope housings and baffles where stray light reduction is vital, and light shields and cold stops in infrared detector assemblies. Black surfaces are used on sources for on-board sensor calibrations and for measurement of spatial nonuniformity of imagers. Passive cooling of infrared systems (detectors, telescopes, electronics subsystems) requires surfaces that are efficient radiators to space. Black surfaces play an important role in the design of infrared seekers used for ballistic missile defense, and for satellite-based surveillance systems. Additionally, target identification requires a database of surface infrared properties.

This article is intended to be a broad review of black surfaces used for purposes such as these, and to provide data to illustrate optical performance. Included are most of the popular surfaces of the hundreds available to designers, as well as new approaches that the reader may find of interest. The data obtained were by this author and by other workers in the field. References are cited for further information and additional data.²

A brief discussion of the uses of black surfaces is found in Sec. II. Detailed descriptions of most of the surfaces cov-

ered in this review are presented in Sec. III, including chemical compositions and process specifications. Section IV discusses substrate preparation.

The measurements are grouped by category: spectrally integrated, hemispherical-directional reflectance in Sec. V; hemispherical emittance by calorimetry in Sec. VI; directional reflectance as a function of wavelength and incident angle in Sec. VII; bidirectional reflectance as a function of wavelength and incident angle in Sec. VIII; and chemical stability (outgassing and atomic oxygen interactions) in Sec. IX.

II. USES OF BLACK SURFACES

A space-borne telescope viewing dim objects must protect against off-axis stray light from the Sun, Earth limb, Moon, as well as from its own housing. This is accomplished by including a baffle assembly to restrict the angular acceptance angle. The design of the baffle needs to very carefully weigh the benefits of diffuse versus specular vane surfaces.³ For example, diffuse surfaces tend to be more susceptible to outgassing and particulate contamination of nearby surfaces than do specular. However, with the specular approach slight design errors or manufacturing tolerances can be more critical.

There can be a difficulty in maintaining the desired knife edge when using paint that can build up on the edge. Some

^{a)}Electronic mail: persky@ll.mit.edu

of the advanced treatments discussed here (black etched beryllium-on-beryllium, plasma sprayed boron-on-beryllium, plasma sprayed boron carbide-on-silicon carbides and plasma sprayed beryllium-on-beryllium) are intended for diffuse-absorptive baffle surfaces that can withstand the mechanical and chemical stability problems of space use and maintain a sharp edge.⁴

Diffuse surfaces in which the energy is absorbed create a further problem, the need to eliminate the heat now being stored in the surface. This requirement, as well as the need to dump heat from electronic units dictates efficient radiators to space, another typical use of black surfaces.

In certain applications the "self" radiation from the telescope or other parts of the instrument can determine the noise level. Cooling to reduce the noise level is typically accomplished by cryogenics which dictates the system will have a limited lifetime. A potential solution is to launch the telescope warm and use black surfaces radiating antisunward to space providing radiative cooling.^{5,6}

The need to verify that the laboratory calibration of a space-borne spectrometer is still applicable during the actual flight leads to the requirement for a space qualified, highly emissive, calibration reference source. In one application the sensor viewed targets deployed from the satellite platform. The solution for this scenario was thus a reference source that would also be deployed from the sensor platform. The source needed to be well characterized, and have a highly stable intensity. The requirement was an absolute intensity accuracy of 15% at any wavelength and 5% when comparing band to band. Also, it should provide useful intensities over three orders of dynamic range.⁷ Use of such an object, if common to several programs, would allow comparisons from flight to flight and to assist in investigating platform or instrument problems.

Since the source is to be deployed into space the sensor signal is due not only to the source self-emission but also to the Solar image and Earthshine reflected from it. Therefore, it is important that the total signal due to source self-emission be maximized and the contributions of reflected Earthshine and Solar image be minimized, a purpose best served by a hemispherical reflectance near zero over the entire sensor band.

The surface chosen for this particular application was the Martin Black. It has a long history of successful space-borne instrument use and provides high emissivity, has minimal spectral features, and is fabricated by a repeatable process.

In one example of use, a 2-cm-diam. sphere was observed for 2000 s during which the signal changed by two orders of magnitude under the influence of day to night illumination changes. Comparing the sensor observation to a model which incorporated the thermal mass and spectral emissivity as well as the environment of upwelling Earthshine, Earth scattered Solar flux and direct Solar flux resulted in mean bias errors ranging from 0.2% to 9%.⁸

It should be noted that many new developments in surface treatments are not as much a result of new applications, but rather that manufacturers have stopped producing certain paints. One example is that of the AVHRR/3 and HIRS/3 meteorological sensors which used 3M401-C10 Black Vel-

vet Nextel paint, one of the industry standards for years before 3M stopped producing this paint. This led to the investigation of Chemglaze Z306 with the addition of glass microspheres to match the 3M performance.⁹

For every application there will be a unique set of specifications: wavelength region, diffuse or specular, resistance to the launch and space environment, manufacturing repeatability, long term storage, and cost. Also, there must be consideration given to optical properties in the visible as many instruments while primarily for the infrared have subassemblies responsive in the visible. Therefore, there probably is no "one fits all" surface treatment.

III. BLACK SURFACE TREATMENTS

A. Composition

The use of a low reflectance surface is intended to control the light impinging on it, to either turn the incident beam into a safe direction, by a specular reflection, or to weaken by diffusing. There are four fundamental mechanisms by which this can be accomplished, operating singly or together:¹⁰

- (a) use of absorbing compounds, by adding, for example, carbon black particles such as in the paints described herein;
- (b) adding large (compared to the wavelength) craters or pits to provide for multiple reflections within the surface, Martin Black being a prime example;
- (c) scattering from the surface structure or substrate; a comparison of gold coatings and anodized coatings over a diffuse substrate with a polished substrate will illustrate this mechanism; and,
- (d) optical interference in thin films to enhance absorption by interference. A limitation of an interference approach is that it can only be used over a very narrow range of angles. To the authors knowledge, interference has not been a primary mechanism for low reflectance space-borne surfaces, although it may be a contributing factor in some.

Surface compositions that utilize these mechanisms for data provided in this review are as follows.

1. *Martin Black*. Per Martin Marietta specification MP30139.

Martin Black is a special proprietary version of an anodized coating. There are four basic steps in the process:¹¹

- (a) vapor hone using aluminum oxide particles to clean the substrate, remove existing oxide, and impart a low frequency roughness component resulting in splash-like craters;
- (b) clean with caustic etch, rinse;
- (c) apply Martin patented (time, temperature, specific gravity) anodize process in a sulfuric acid bath;
- (d) immerse in Nigrosin dye for a controlled time and temperature, and hot water seal to close the pores (processing details Martin proprietary).

This process results in a surface with roughness of 8 μm and thickness of approximately 75 μm (with a variability of

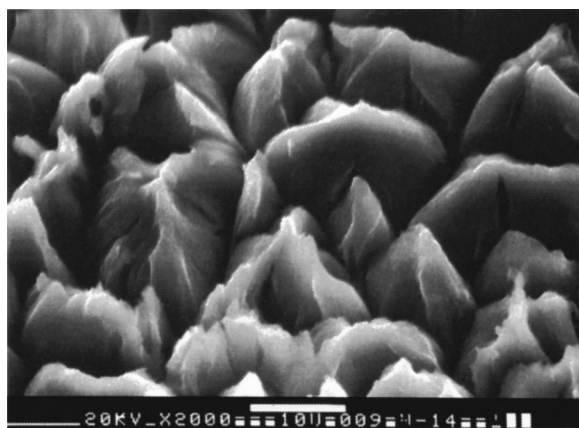


FIG. 1. SEM photograph of Martin Black surface structure. Horizontal white bar is 10 μm long.

at least $\pm 20 \mu\text{m}$).¹² While the exact chemistry of the anodized surface is unknown, the specific absorption mechanisms appear to include both electromagnetic and cavity effects:

- (a) low frequency craters resulting from the vapor honing process,
- (b) high frequency pits resulting from the anodize process with the peaks formed by the anodization being closer together than the craters formed by the vapor honing,
- (c) faults within the high frequency anodized aluminum pits that are created as a result of the anodizing process,
- (d) optical constants of the surface resulting from the anodizing and sealing process,
- (e) optical constants of the Nigrosin dye.

The surface character is seen in the scanning electron microscopy (SEM) photograph in Fig. 1. The cavities act as light traps to minimize the reflectivity and, hence, increase the emissivity of the substrate. However, at the same time the peaks are very susceptible to fracture making the surface fragile to the touch.

Martin Marietta also produces variants of Martin Black; Infrablack, which is blacker in certain spectral regions than Martin Black due to a change in the dye as well as greater roughness;^{13,14} and Enhanced Martin Black and Enhanced Infrablack which are especially resistant to chemical and atomic oxygen attack.¹⁵ Infrablack has had the aluminum substrate first roughened by a hexagonal array of 1/64-in.-diam. holes before application of Martin Black.¹⁶ Enhanced Martin Black is sealed in steam after dyeing rather than water.¹⁷ Availability: Martin Marietta Astronautics Group (D.Shepard[donald.f.shepard@lmco.com]), Denver, CO.

2. *Black anodize*. Per MIL-A-8625, class 2, type II (sulfuric acid bath at 72F, Sandoz aniline dye, Sandofix nickel acetate). Availability: Commercial plating companies.

3. *Black Hardcoat*. Per MIL-A-8625, class 2, type III (sulfuric acid bath at 26F, Sandoz aniline dye, Sandofix nickel acetate sealer). Originally developed by Martin Aircraft Co. for aircraft wing surface. Availability: Commercial plating companies.

4. *Black Hardlub*. Per MIL-A-8625, class 1, type III (sulfuric acid bath at 26F), Dupont VYDAX WD soak con-

taining Teflon spheres impregnated into the surface. Availability: Commercial plating companies.

5. *Ebanol C*. Per MIL-C-14550 (undercoat) and MIL-F-495 processes: immersion in a zincate bath followed by a high cyanide, low copper bath, and copper strike and dip in an Ebanol C solution. Availability: Commercial plating companies.

6. *Sikkens (Akzo) No. 463-3-8B paint* (also known as Finch, Bostik and Cat-A-Lac). Epoxy amine flat black with CA-103 amine catalyst. Pigment is 1.7% carbon black, 28% magnesium silicate. Vehicle solids are 23.3% epoxy resin. Availability: Akzo Coatings, Inc., Orange, CA.

7. *Eccosorb 268E paint*. Hydrocarbon epoxy resin. Pigment is >60% bisphenol a/epichlorohydrin and mineral fillers. Used as a radar absorbing paint, electrically nonconductive. Availability: Emerson and Cuming Microwave Products, Randolph, MA.

8. *Chemglaze Z306 paint (now known as Aeroglaze Z306)*. Aromatic polyurethane flatblack with No. 9924 primer. Pigment is <5% carbon black, silica, and urethane resins.

Commercial paint originally formulated to resist extensive mechanical wear on wood floors and boat decks. A special formulation includes microspheres to increase diffuse reflection. Availability: Lord Corporation, Erie, Pa.

9. *Parsons Optical Black lacquer*. Undercoat is nitrocellulose lacquer pigment, 2% carbon black, 41% ethyl cellulose resin. Topcoat is 4% carbon black pigment, 12% ethyl cellulose resin.

The National Physical Laboratory, London originally developed this paint for blackening radiometer detector surfaces.

Not currently available; previously from Eppley Laboratory, Newport, RI.

10. *AMES 24E paint*. Ethyl silicate paint (ECP-2200) loaded with No. 80 silicon carbide grinding grit and carbon black.¹⁸ Availability: Contact S. Smith, 408-378-9779.

11. *Teflon-Dupont Grade 7A (polytetrafluoroethylene polymer)*. Low reflectivity by the mechanism of bulk absorption. Samples were cut from sheet stock, surface as manufactured. Availability: Commercial suppliers.

12. *Ball IR Black (BIRB)*. DeSoto Black binder plus silicon carbide grinding compound and carbon black.

The surface consists of surface facets appearing as tall, columnar shaped spikes. Availability: To be determined. Courtauld's Aerospace is no longer the manufacturer of DeSoto Black and it is not known if it will be continued by some other manufacturer.¹⁹

13. *Appliqués*. Appliqué refers to a freestanding sheet of material attached to a substrate with an adhesive.²⁰ This review includes data for five such surfaces: a Battelle appliqué; two from Energy Science Laboratory, Inc. (ESLI); black Kapton; and one developed at the Naval Research Laboratory (NRL) called R/F aerogel.

The Battelle surface uses a carbon loaded polyurethane film with a surface heat molded into a microgroove pattern. The ESLI surface consists of high aspect ratio fibers mounted with a black epoxy adhesive on to an aluminum substrate. The other ESLI treatment discussed here is a "bi-

ased" coating in which the carbon fibers are tilted approximately 30°–35° relative to the base. The *R/F* aerogel results from reacting resorcinol and formaldehyde in the presence of a catalyst to form a cross-linked polymer gel. This gel is then heated at 1015 °C in an inert atmosphere to pyrolyze the structure, thus forming a carbon aerogel.²¹

Two of the advantages of appliquéés over other black surface are that, in certain situations, the scattering is lower than for conventional diffuse black surfaces, and they are easily applied. The two main disadvantages for space use are outgassing and atomic oxygen exposure levels which may be unacceptable. However, there is an ongoing effort to space qualify the CLSA96/1. Availability: from several organizations (see Ref. 20)

14. *Ion Beam Textured*. Process is designed to microscopically texture metal surface with pores and cones using deliberately introduced seed atoms.²²

Ion beam texturing provides surfaces which are both rough and very rugged, a normally difficult combination. Broadband absorbers can be created with a random mixture of both large and small features which provides multiple scattering from the different size features. If the features are small and of uniform size a specific narrow band can be provided. Feature size is controlled through surface temperature, gasses in the vacuum chamber during ion bombardment, seed metal, beam species, energy, and current density. Availability: see Ref. 22

15. *Black Chrome*. Electrodeposited using chrome and chromium oxides on titanium.²³

This is an example of a surface which is diffuse black in the visible and specular in the infrared. Availability: Martin Marietta Astronautics Group (D. Shepard [donald.f.shepard@lmco.com]) Denver, CO.

16. *Advanced Optically Black Diffuse Surfaces*. Black etched beryllium-on-beryllium, plasma sprayed boron-on-beryllium, plasma sprayed boron carbide-on-silicon carbide, and plasma sprayed beryllium-on-beryllium, are diffuse-absorptive surfaces that employ microscopic structures to absorb, scatter, or trap light.²⁴ The intent is to provide a surface which has no specular component greater than the scatter properties.

Specifications are that the surface structure has an aspect ratio of 3 to 10 times the wavelength and that the feature size be comparable to or slightly smaller than the wavelength. The pores need to be comparable to or slightly greater than the wavelength to be effective. One concern is the potential for particle generation during launch vibration. Availability: See Ref. 24.

B. Space flight history

A compilation of surfaces actually used or proposed for use on space-borne instruments is given in Table I. Several surfaces were described previously in Sec. III A. The remaining are as follows:

1. *Eccosorb CR-110*. This is a castable epoxy resin material that is naturally black. It's available from Emerson and Cuming Microwave Products, Randolph, MA.

2. *Astro Black* was developed by Nippon Paint Co., in Japan.²⁵

3. *DeSoto Black* is a flat black paint ideal for use in the near infrared with a reflectance of 2% to 3% in this region, thus the choice for the Near Infrared Camera and Multi-Object Spectrograph (NICMOS) on the Hubble telescope.²⁶ The 300 K weighted emissivity is 0.96 and solar absorptivity is 0.924. The outgassing weight loss is below 0.5% and volatile condensable material is also below 0.5%.

4. *MSA94B* is a black silicate paint having a diffuse emissivity of 0.89.²⁷ It was developed at NASA Goddard Space Flight Center.

5. *MAP PSB* is a nonconductive, white silicate paint having a hemispheric emissivity of 0.88.²⁸ It is one of several paints manufactured by MAP of Pamiers, France and has been used on Meteosat, DFS and others. Outgassing properties are: a total material loss of 2.82%, and collected volatile condensable materials of 0.004%, which compare well with the Chemglaze Z306 paint.

6. *Berkeley black* was developed by Bock to use as a submillimeter coating for a cooled telescope baffle system.²⁹ The composition by mass is: 68% Stycast 2850FT (Emerson & Cuming, Inc., Woburn, MA); 5% Catalyst 24LV; 7% Carbon Lampblack; 20% 175- μ m-diam. Glass Beads (Size No. 100, Fuji Manufacturing Corp., Edogawa, Tokyo 132, Japan).

The composition can be varied depending on the absorptivity required for the wavelength and application, and the glass beads that serve to roughen the surface can be omitted if not required. The amount of lampblack can be lowered to improve the handling (viscosity is reduced) but with a reduction in absorptivity.

Measurements of the index of refraction ranged from 2.00 for a 80% Stycast, 20% glass beads mix, to 2.80 for the 73%, 7%, 20% mix given above. The absorption coefficients for this typical composition range from 10 per cm at 10 cm^{-1} to 230 per cm at 60 cm^{-1} . The reflectances of 0.1 at 10 cm^{-1} and 0.025 at 60 cm^{-1} compare favorably with those of the Ames 24E paint. Vibration testing of a telescope baffle design was conducted at liquid nitrogen temperature with favorable results. The coating has been used in two rocket-borne instruments.

7. *Chemglaze Z307* is an electrically conductive version of Chemglaze Z306.

IV. SUBSTRATE PREPARATION

Preparation of the substrate and surface application methods can both have a significant impact on the reflectance and robustness of the final surface.

An important precaution that should be taken is the removal of machine oil left in mounting holes. This oil can leach to the surface causing a discoloration. Typical substrate cleaning includes vapor degreasing, ultrasonic cleaning with an organic solvent, and water and alcohol rinse.

TABLE I. Black surfaces used on space-borne instruments.

Surface	Satellite	Sensor	Use	Ref.
Martin Black	Galileo Probe	Nephelometer, Net Flux Radiometer		65
	Spacelab 2	IR Telescope		65
	Giotto	Particle Impact Analyzer		66
	IRAS	Telescope		65
	Space Shuttle	Star Tracker	Sun Shields	65
	Hubble Space Telescope			67
	Landsat	Thematic Mapper	Baffles	68
Enh, Martin Black	ENVISAT ^a	MIPAS	BB Calibrator	69
	ERS-1, ERS-2, ENVISAT ^a	ATSR	BB Calibrator	70
EBANOL C	Clementine	UV/Vis Camera	External Baffle	71
	Clementine	Star Tracker	Baffle	72
Chemglaze Z306	MSX	Spirit III	Telescope Baffles	73
	EO-1 ^a	Advanced Land Imager	Housing	74
	UARS	CLAES		73
	Hubble Space Telescope			67
	ENVISAT ^a	MIPAS	Baseplate	69
	Mars 96	PFS	Long Wave Channel Housing	75
	GOES	Imager, Sounder	Internal Cal. Targets	76
	POES	AVHRR/3, HIRS/3	Internal Cal. Targets	76
	Landsat 4, 5, 6, 7	Thematic Mapper		68
	EOS-AM ^a	MODIS		68
	Small Explorer Series ^a	WIRE		77
Chemglaze Z306+ μ Spheres	GOES	Imager, Sounder	Telescope Baffles	76
	POES	AVHRR/3	Telescope Baffles	76
Chemglaze Z302	GOES	Imager, Sounder	Telescope Baffles	76
Chemglaze Z307	GOES	Imager, Sounder	Radiators	76
Sikkens 463	LES			
	GOES 1-3	VISSR		68
	GOES 4-7	VAS		68
	Landsat 1-5	MSS		68
	Pioneer	IRR		68
	Pioneer	IPP		68
	Hubble Space Telescope			67
Sikkens 443	Hubble Space Telescope			67
Parsons	OSO III			
Ames 24E	SIRTF ^a		Baffle	78
CTL-15	EOS AM-1 ^a	MODIS	BB Calibrator	68
Black Anodize	EOS AM-1 ^a	MODIS	BB Calibrator	68
	Clementine	Long Wave IR Camera	Lens Housing	79
	Clementine	Near IR Camera	Lens Housing	80
	Clementine	UV/VIS Camera	Internal Baffles	71
	COBE	DIRBE	Baffle	81
	ENVISAT ^a	MIPAS	Miscellaneous	69
	Mars 96	PFS	Interior	75
	Small Explorer Series ^a	WIRE	Electronics Box	77
	COBE	FIRAS	BB Calibrator	81
	ADEOS	IMG	IMG Structure, Electronics Box	82
	DeSoto Black	Hubble Space Telescope	NICMOS	Baffles
MSA94B	CASSINI	CIRS	Telescope, Baffles, Sunshade	81
MAP PSB	MARS 96	PFS	Thermal Control	75
Berkeley Black	Space Flyer Unit	IRTS	Telescope Baffle	84
Navord Alodine	HST	COSTAR	Mechanical Structure	85

^aFuture launch.

Aluminum substrates to be used for paints are also Alodined to insure adhesion. Alodine is a chemical containing acidic chromates and fluorides to make the aluminum impervious to oxidation.

A significant preparation issue for paints is that of coating uniformity over the entire surface. This can be a particu-

lar problem for nonflat substrates. One method is electrostatic spray, a commercial technique commonly used for nonflat objects. Electrostatic spraying can be a viable approach except that not all paints are designed to be applied by electrostatic spraying, thus inconsistent application of both primers and undercoats can occur.

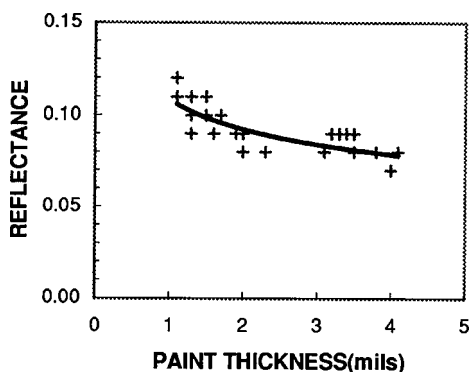


FIG. 2. Chemglaze Z306 reflectance vs paint thickness. Reflectance is constant for thickness exceeding 3 mils. (DB-100 measurement).

For flat samples high-pressure air spray can usually provide a uniform thickness. The important precaution is to insure that there is sufficient paint thickness to provide absorption before any rays reach the substrate. If the substrate is sandblasted and anodized prior to painting then paint adherence is enhanced, and a low reflectance (0.13) layer is provided beneath the paint in the event marring of the surface takes place.

A typical relationship between reflectance and paint thickness is given in Fig. 2 for Chemglaze Z306. The results indicate that the reflectance is a weak function of coating thickness. This implies that manufacturing tolerances can be fairly wide so long as the paint is sufficiently thick that the substrate would not contribute to the signature. Bear in mind that excessive paint can create unnecessary outgassing problems.

V. 5 TO 25 μm , SPECTRALLY INTEGRATED, HEMISPHERICAL-DIRECTIONAL REFLECTANCE

These data are obtained by relatively simple, easy to operate instruments, thus are a cost-effective approach for initial evaluation of surfaces. Since the data represent spectrally integrated values ideally for gray surfaces, care must be taken in the interpretation of surfaces having significant spectral structure.

A. Instrumentation

The spectrally integrated, hemispherical-directional reflectance is provided by a Gier-Dunkle DB100 Infrared Reflectometer, models of which were operated by this author; by Henninger (NASA Goddard Space Flight Center), and by Sampair (NASA Langley Research Center).

Specifications are provided in Table II. The instrument utilizes hemispherical input, near-normal output. A rotating cylinder with two cavities alternatively irradiate the test specimen with 32 and 43 °C blackbody radiation while a thermopile detector at 7° from normal generates a modulat-

TABLE II. Gier Dunkle DB100 infrared reflectometer used for 5–25 μm , hemispherical-directional reflectance.

Illumination	$\pm 52^\circ$
Detection	narrow beam at 7° from normal
Reflectance	hemispherical input-directional output
Spectral range	5–25 μm
Accuracy	0.01–0.03 ^a
Precision	± 0.002

^aEstimated for nongray surfaces.

ing signal proportional to the reflectance of the sample. Polyethylene film with carbon black is used in conjunction with the two black bodies to shape the response such that the incident energy approximates a 25 °C blackbody, integrated over a 5 to 25 μm response.

The instrument is calibrated using 3M black velvet tape and gold coated brass standards provided by the manufacturer. These are flat standards applicable to flat surface specimens only. For nonflat substrates a correction is necessary. The author has used a set of planoconvex substrates covering a range of curvatures, coated with evaporative gold. From the reflectivity readings a correction factor was determined for use with nonflat surfaces.

The reflectance accuracy is quoted by the manufacturer as between ± 0.02 and ± 0.03 units depending on the spectral content. The reflectance precision is estimated from this author's measurements to be < 0.010 units.

B. Discussion

Hemispherical-directional reflectance values obtained by this author are given in Table III in terms of mean and standard deviation. Along side for comparison are values (also averages) obtained by Henninger. The close match serves to give confidence to the results.

TABLE III. Mean values of 5–25 μm , near-normal, hemispherical-directional reflectance. Differences due to substrates are indicated.

Surface	Henninger (Ref. 86)	This author	Std. dev.	No. of samples
Martin Black	...	0.05	0.005	15
Parsons Black ^{a,b}	0.09	0.08	0.004	21
Chemglaze Z306 ^{a,b}	0.09	0.09	0.005	26
Teflon	...	0.09	0.005	4
Sikkens 463 ^{a,b}	0.12	0.11	0.007	24
Eccosorb 268E ^{a,b}	...	0.11	0.005	19
Black Anodize ^a	0.12	0.12	0.006	5
Black Anodize ^b	...	0.15	0.005	5
Black Anodize ^c	...	0.17	0.002	3
Black Hardcoat ^a	...	0.13	0.010	10
Black Hardlub ^{a,b}	...	0.14	0.002	6
Ebonal C ^a	0.27	0.28	0.023	8
Ebonal C ^b	...	0.32	0.080	13
3M Nextel	0.09	0.08	...	2
Evaporative Gold	0.98	0.99	0.005	6

^aOn sandblasted substrate.

^bOn raw substrate.

^cOn polished substrate.

Using the mean as indicator we see that the Martin Black has the lowest reflectance and the standard deviation indicates excellent manufacturing reproducibility. The data set includes samples made at five different times over a two year period. Note also that Sampair and Berrios measured the reflectance of a Chemglaze Z306 sample to be 0.08 on a sample that had been on the Long Duration Exposure Facility for 5 3/4 years in low Earth orbit.³⁰

Next in increasing reflectance are Teflon and two paints, Parsons Black and Chemglaze Z306. They have nearly identical reflectances within the overall accuracy of the measurements. Notice that the paints also have extremely good reproducibility, especially given that they were produced in several sets over time periods as long as 10 months.

The three versions of conventional anodizing are fairly similar. The influence of the substrate is seen with the black anodize data. The standard deviations indicate best reproducibility for the Hardlub.

The Ebanol group not only has poor reflectivity within this band, but unacceptable sample-to-sample uniformity. The problem may be in the control of the copper oxide thickness, which can have a significant impact on the reflectance. The substrate used by Henninger for Ebanol C is not known, but it is assumed sandblasted given the best match to this author's data.

Long term stability is indicated by review of repeated measurements on the same sample after an elapsed time of as much as a year or more. Table IV presents data for several of the surfaces. In all cases the repeated measurement was statistically identical to the original.

VI. HEMISPHERICAL EMITTANCE BY CALORIMETRY

A nonoptical method for emittance determination is the calorimetric approach. Measurement is made of the surface temperature as a function of time while the surface radiates to the black, cold (<-160 °C) walls of a vacuum chamber. Since the time rate of change of temperature as the surface radiates to a colder environment is dictated by its total hemispherical emittance, iteration of the time rate with a thermal model can be used to extract the emittance.

TABLE IV. Repeat measurements of 5–25 μm, hemispheric-directional reflectance to judge long term stability. Samples stored under room conditions.

Surface	Original measurements	Elapsed time (Months)	Repeat measurement
Martin Black	0.06	15	0.05
	0.05	11	0.05
Parsons Black	0.08	12	0.07
Chemglaze Z306	0.11	15	0.11
Black Anodize	0.14	13	0.13
Black Hardcoat	0.14	17	0.13

The relationship between time and surface temperature for an isothermal object radiating to a zero background environment is

$$T = T_0 / [1 + t/\tau]^{1/3}, \tag{1}$$

where,

$$\tau = C_p \rho b / 9 \epsilon_{\tau,h} \sigma T_0,$$

T_0 = initial temperature,

T = final temperature,

C_p = specific heat,

ρ = density,

b = radius of sphere,

σ = Stefan-Boltzman constant

$$(5.710^{-12} \text{ w/cm}^2 \text{ deg}^4),$$

$\epsilon_{\tau,h}$ = total hemispheric emittance.

The results of a test on a 3 in. diameter, Martin Black coated aluminum sphere are shown in Fig. 3. The profile of temperature decrease versus time matches the theoretical profile for a 0.94 emissive surface over the range from 250 to 340 K. A calorimetric measurement of a second Martin Black sphere produced some 5 years later resulted in an emittance of 0.95–0.96, with an uncertainty of 0.008. The emittance was constant over a 200–325 K surface temperature range.³¹

VII. SPECTRAL, HEMISPHERICAL-DIRECTIONAL REFLECTANCE

The majority of black surfaces are not gray, but rather, the reflectance can vary widely over a broad range of wavelengths. It is important to the performance of a surface for it to be optimized for the wavelength of use. Spectral, directional reflectance measurements are used to provide the spectral signatures.

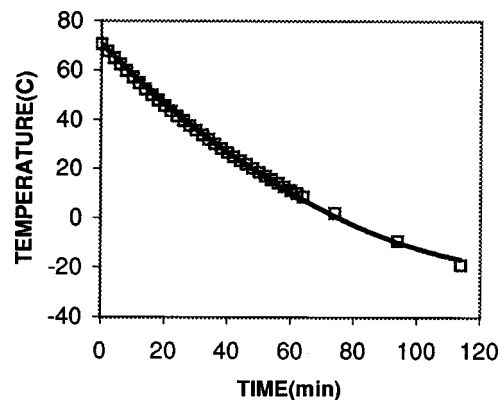


FIG. 3. Calorimetric measurement of temperature-time history for a Martin Black sphere radiating to 77 K background. Comparison to thermal model of temperature vs time indicates a hemispherical emissivity of 0.94.

A. Instrumentation

The spectral measurements in this section were made by six different systems.

1. Figures 5–10, 14–19, and 21–24

Spectral reflectance measurements, total and diffuse only, were made by Surface Optics, Corp. (SOC) for this author. Because of the large expense involved in extensive absolute spectral measurements, the author, using a Perkin–Elmer 983 Spectrometer obtained a precursor set of relative spectral reflectance data. These data are contiguous from 2.5 to 25 μm . The particular wavelengths at which significant spectral features appear were then the specific wavelengths for the absolute reflectance measurements.

Salient characteristics of the SOC directional reflectometer (DR) are provided in Table V and the instrument is illustrated in Fig. 4.³² An incident angle of $\theta_1 = 20^\circ$ represents near normal while 60° is significantly off normal. The data in these figures were all at an incident azimuth angle of 0° .

The instrument is a hemiellipsoidal reflectometer coupled to a Perkin–Elmer Model 210 grating monochrometer. A hot source located at one focus hemispherically irradiates the sample located at the other focus. The reflected beam at selected angles is then directed to the monochrometer. By reciprocity, the measurement is considered identical to illumination from a specific incident angle with uniform detection of all the radiation reflected by the sample into the hemisphere.

The instrument is designed such that a blocker can be inserted in the beam between source and sample to prevent the specular reflectance from being included. This is then the diffuse reflectance. Data provided herein are both directional (specular plus diffuse) and diffuse only. The grating is moved step by step to provide a point by point wavelength “scan.” Because the grating polarizes the radiation, a pair of measurements is made using a polarizer oriented to measure both the parallel and perpendicular components from which the average reflectance is computed. The 100% reflectance

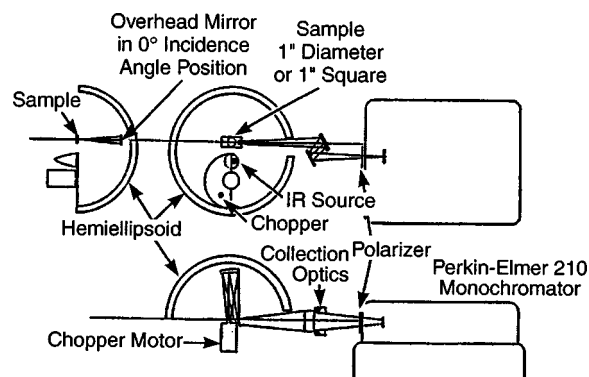


FIG. 4. Surface Optics, Corp. spectral, directional reflectance instrument. Overhead mirror is rotated to vary the incident angle. Sample, chopper, source rotate; collection optics, and monochromator remain fixed. (After Ref. 32.)

calibration level used fused silica (Spectrasil B from Physitex, Inc.) as a standard, derived from the known indices of refraction of this specular material.

Figures 5 and 6 are spectra obtained by the SOC DR to serve as high signal to noise, instrument performance references for comparison to the data to follow. The Labsphere DSP 200 is an electrochemical gold plating on a sandblasted aluminum substrate. It provides a high reflectance, graybody spectrum with diffuse scattering. For specular reflecting surfaces, a reference was constructed by grinding a disk of 6061-T6 aluminum; plating of 2 mils electro-optical nickel; fine polish; and electrolytic plating of type III gold.

TABLE V. Surface Optics Corp. spectral, directional reflectance instrumentation.

Type	hemiellipsoidal reflectometer
Operation	hemispherical illumination, directional detection directional reflectance by reciprocity
Spectral resolution	0.256 μm at 5 μm 0.229 μm at 10 μm 0.173 μm at 15 μm 0.595 μm at 20 μm
Incident angle accuracy	$\pm 5^\circ$
Reflectance accuracy	near normal to 70° ± 0.01 > 70° ± 0.03
Source beam width	3.4°
Monochromator	Perkin–Elmer Model 210 grating

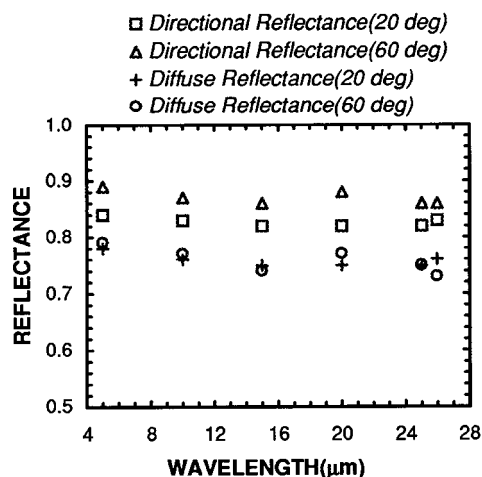


FIG. 5. Directional (specular plus diffuse) and diffuse only spectral reflectance of Labsphere, Inc. DSP 200 electrochemical gold coating for 20° and 60° incident angles. Substrate is sandblasted aluminum with $6 \mu\text{m}$ arithmetic average roughness.

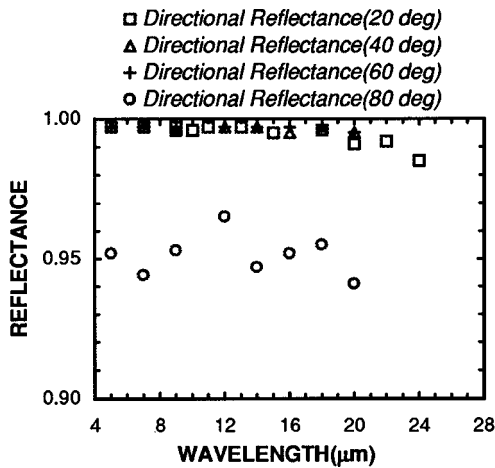


FIG. 6. Directional (specular plus diffuse) spectral reflectance of electrolytic gold plating (10 μm inches of type III) on polished and nickel-plated aluminum substrate. Decrease at 80° incident angle is as predicted by electromagnetic theory.

2. Figures 11 and 12

A Beckman IR-3 prism spectrophotometer was used at the Naval Command, Control and Ocean Surveillance Center (NCCOSC) to produce the emittance measurements of surfaces from 77 to 315 K. Unwanted scattered radiation is attenuated to less than one part in one million to insure spectral purity. The instrument is fully evacuated and temperature controlled by a 25 °C water bath. The emission from the sample is chopped against a 25 °C blackbody. The signal is then compared to a second calibrated cavity blackbody substituted in place of the sample.³³

Additionally, a Surface Optics Corp., SOC-100 Hemispherical Directional Reflectometer was used by SOC for Fig. 12.³⁴ It is essentially the same as the instrument described in Sec. VII A 1 except for the replacement of the grating monochromator with a Nicolet 550/750 Fourier transform infrared (FTIR) spectrometer. Uncertainties are estimated to be 1%(1σ).

3. Figure 13

Smith used a nonspecular reflectometer photometer-goniometer for both spectral, directional reflectance, and bi-directional reflectance-distribution function (BRDF).³⁵ The source is a 1273 K blackbody located at an angle, θ_1 , to the surface normal. An ellipsoidal mirror reflects the source to the sample. The reflected energy from the sample is focused onto the detector that is located at an equal angle, θ_1 , on the other side of the normal. This is the specular reflection. The detector assembly contains wavelength-defining filters to provide the spectral definition. A smooth, gold-coated surface provides the calibration for both directional reflectance and BRDF. The detector acceptance solid angle for the specular reflectance is $8.94e-4$ steradians.

4. Figure 20

These diffuse reflectivity data were obtained by Harrick Scientific (Ossining, NY) for Ames.³⁶ The reflectivity calibration uses roughened aluminum as standard.

5. Figure 25

An integrating sphere reflectometer coupled to a Digilab Fourier transform infrared spectrometer (FTIR) was used for this spectral directional-hemispheric measurement at the National Institute of Science and Technology (NIST).

B. Discussion

1. Martin Black, Infrablack, Enhanced Martin Black

Figures 7–13 are spectral reflectance data pertaining to Martin Black, Enhanced Martin Black, and Infrablack.

Figure 7 indicates that at near normal (20°) the Martin Black directional reflectance is dominated by the diffuse component of the reflectance. Figure 8 provides reflectance versus incidence angle indicating a significant increase with incidence angle. Figure 9 presents reflectance for five samples in a common batch, demonstrating excellent manufacturing repeatability. Furthermore, as shown in Fig. 10, samples produced over a seven-year period likewise are very similar, as expected from a well defined and maintained manufacturing process.

It results from adsorbed water on the surface. In this spectral region the imaginary part of the index of refraction is sufficiently large that Fresnel's equations indicate strong reflectance peaks.³⁷

Figure 11, by Shumway *et al.*, is a set of measurements of Martin Black at surface temperatures of 77, 200, and 315 K. Prior to these measurements, the sample was held at 315 K in a $10e-3$ Torr vacuum to outgas. There is a slight reflectance variation at 7 μm for the temperature change from 77 to 200 K but none to 315 K greater than the measurement accuracy. The 8–24 μm reflectance did not evidence any temperature dependence.³⁸

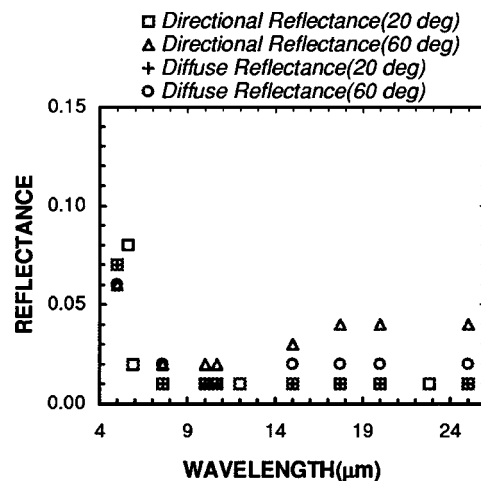


FIG. 7. Martin Black directional (specular plus diffuse) and diffuse only spectral reflectance. Note restrahlen peak at 5 μm.

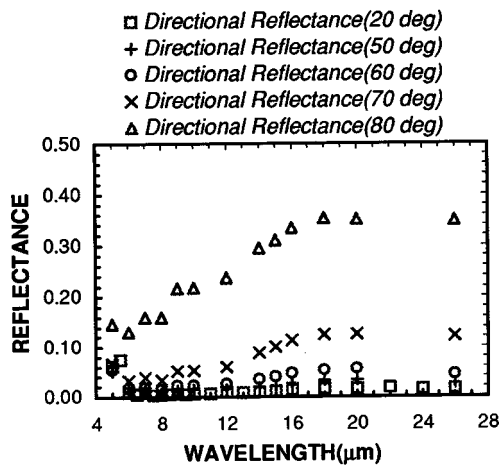


FIG. 8. Martin Black directional (specular plus diffuse) spectral reflectance as a function of incident angles. Dramatic increase in reflectance is seen at near-grazing incidence.

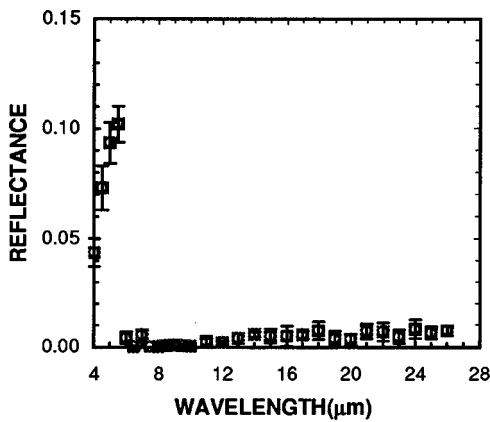


FIG. 9. Martin Black directional (specular plus diffuse) spectral reflectance at an incident angle of 20° for five samples in one manufacturing batch. Excellent repeatability is demonstrated.

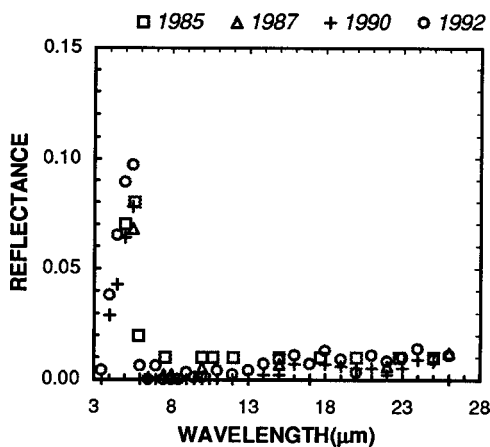


FIG. 10. Martin Black directional (specular plus diffuse) spectral reflectance at 20° incident angle. Nearly identical reflectances of four samples manufactured over a seven year period indicates advantage of a specified manufacturing process.

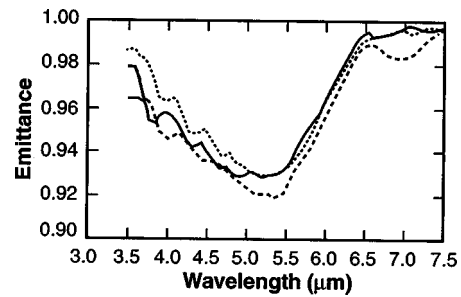


FIG. 11. Martin Black directional emittance in the region of the 5 μm emittance minimum (restrahlen reflectance peak). Incident angle is 0°. Surface temperatures were 315 (dashed), 200 (solid), and 77 K (dotted). (After Ref. 38.)

Figure 12 is the directional emittance for an Enhanced Martin Black sample likewise held at 315 K in a $10e-3$ Torr vacuum to outgas. No temperature dependence from 77 to 315 K is observed and the measurements compare well to the ambient temperature measurement included. What is most noteworthy is the reduction in the peak at 5 μm seen with the Enhanced version. Martin Black is sealed in water while Enhanced is sealed in steam which contributes to the difference.

Additional measurements of both surfaces are presented in Ref. 38 for a variety of temperatures from 77 to 620 K, with various vacuum exposure and humidity conditions.³⁹

Smith compares far-infrared spectra for Martin Black, Infrablack, and Ames 24E paint in Fig. 13.⁴⁰ Note that at this course resolution, only general trends in the spectra are shown. The result of the greater surface roughness of Infrablack is a reduction in reflectance as compared to Martin Black. Also, Ames 24E has 1 to 2 orders of magnitude less reflectance than the others.

2. Black Anodize, Black Hardcoat, Black Hardlub, and Ebonal C

Figures 14–18 provide the directional and diffuse reflectance spectra for the rest of the electrochemical treatments in this review. It is notable that the anodize, Hardcoat, and Hardlub family, exhibit similar signatures to the Martin Black, especially the peak in the 3–6 μm region.

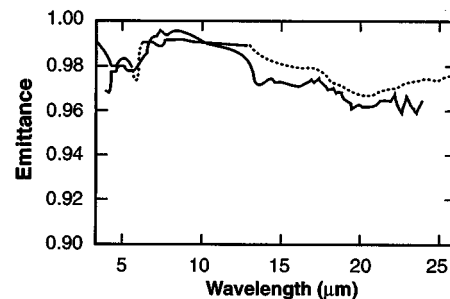


FIG. 12. Enhanced Martin Black directional emittance (solid line) averaged over 77, 200, and 315 K measurements. Directional reflectance measurements converted to emittance compare well (dotted lines). Incident angle is 0°. (After Ref. 39.)

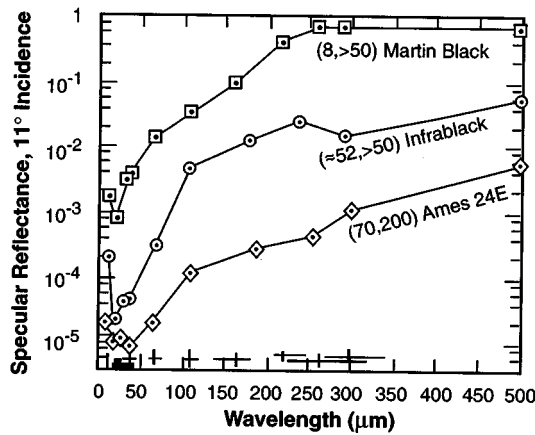


FIG. 13. Martin Black, Infrablack, and Ames 24E specular reflectance comparison. The first value in the parenthesis is the root-mean-square (rms) roughness (μm), the second the thickness (μm). Crosses just above the abscissa indicate error estimates and filter pass bands. The detector solid angle is $8.94 \times 10^{-4} \text{ ster}^{-1}$. (After Ref. 40.)

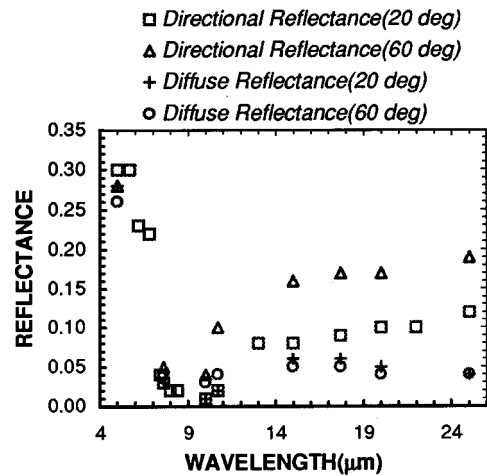


FIG. 16. Black Hardlub directional (specular plus diffuse) and diffuse only reflectances. Substrate was raw, stock aluminum. Diffuse reflectance is constant vs incident angle.

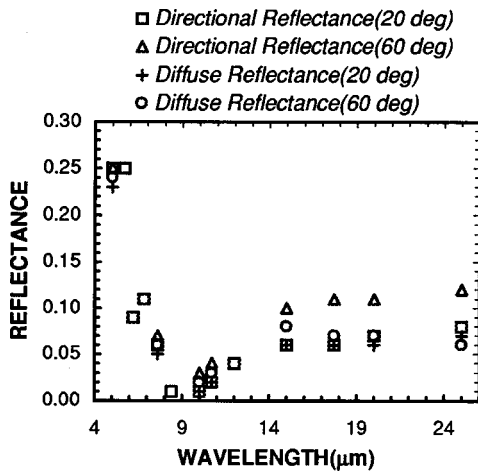


FIG. 14. Black anodize directional (specular plus diffuse) and diffuse only reflectances. Surface was sandblasted prior to anodization. Reflection is primarily diffuse at a 20° incident angle.

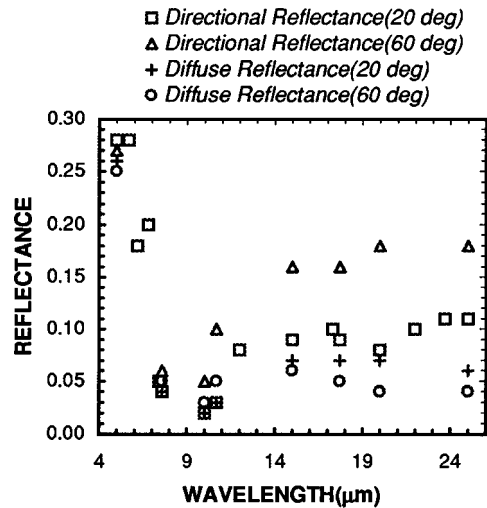


FIG. 17. Black Hardcoat directional (specular plus diffuse) and diffuse only reflectances. Substrate was sandblasted. Reflectance is similar to that of the other anodizes. Note in particular the $5 \mu\text{m}$ reststrahlen peak that appears in all the anodized surfaces as well as the Martin Black.

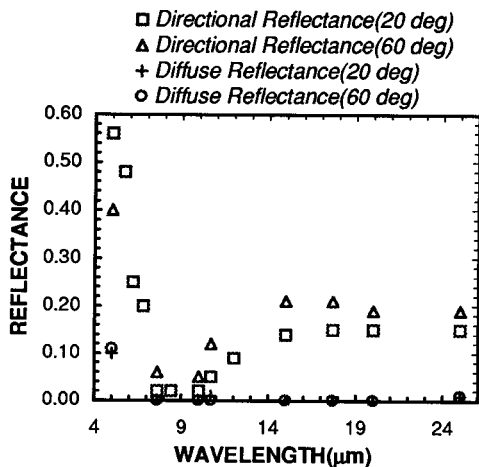


FIG. 15. Black anodize directional (specular plus diffuse) and diffuse only reflectances. Surface was polished prior to anodization. Reflection is primarily specular.

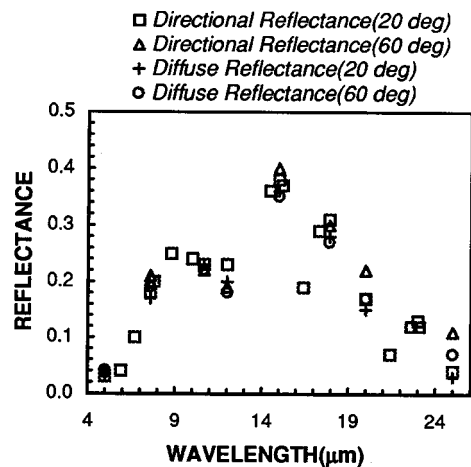


FIG. 18. Ebonal C directional (specular plus diffuse) and diffuse only reflectances. Treatment applied to sandblasted substrate. Reflectance is predominantly diffuse at all wavelengths.

Comparing the black anodize on a sandblasted substrate (Fig. 14) with that on a polished substrate (Fig. 15) indicates a factor of two higher reflectance and significant reduction in the diffuse component due to the influence of the substrate. The Ebonal C is significantly nongray (Fig. 18), and is extremely diffuse. This is seen in the BRDF as well (Fig. 41 to follow).

3. Paints

The paint-on surfaces (Figs. 19–23) exhibit a variety of characteristic spectral signatures. The Chemglaze Z306 spectrum by Ames (Fig. 20) is on an expanded reflectance scale thus for most purposes it can be described as a gray surface.⁴¹ The impact of the addition of microspheres is clearly seen leading to its possible substitution for the previously used Black Velvet Nextel. However, this enhancement is limited to surfaces not likely to suffer high vibration levels which could “shake out” the microspheres.

The Sikkens 463 and Eccosorb 268E have somewhat nongray signatures which reduces their usefulness for use as broad band coatings while the Parsons Black is fairly featureless (Figs. 21–23).

4. Teflon

Teflon (Fig. 24) has fairly low reflectance over most of the 5–25 μm range except for two regions near 9 and 20 μm . The diffuse reflectance is extremely low such that the specular component dominates.

5. Appliqués

Figure 25 provides a comparison of two appliqués with Martin Black.⁴² The incident angle was 8° for these directional-hemispheric data. Both appliqués are devoid of any spectral structure in the 2–13 μm region and the hemispherical reflectance of 1% and less is quite impressive.

6. Advanced optically black surfaces

Seals and McIntosh give the specular reflectances of four advanced optically black materials in Fig. 26.⁴³ The spectral reflectances are gray but not to the low level of the baseline Martin Black.

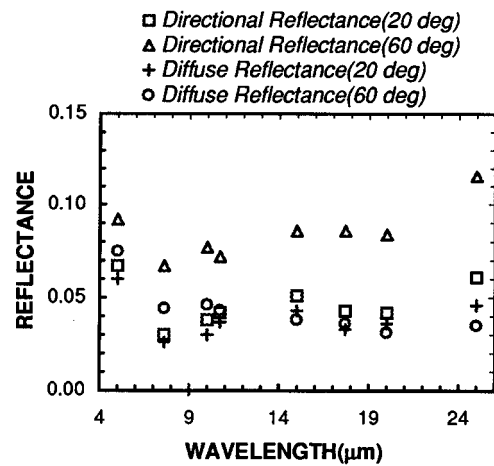


FIG. 19. Chemglaze (Aeroglaze) Z306 paint directional (specular plus diffuse) and diffuse only reflectances. Reflectance is graybody, with significant increase in specular reflectance at 60° incident angle. Substrate was raw stock aluminum.

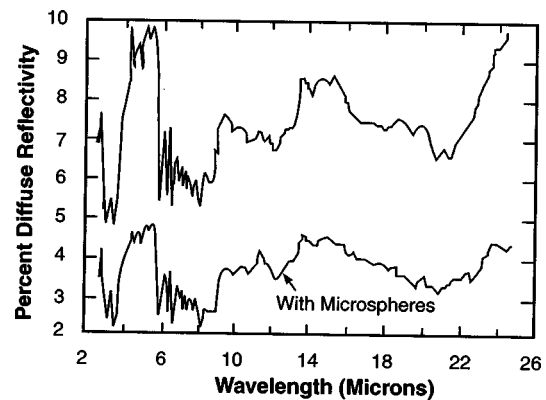


FIG. 20. Chemglaze (Aeroglaze) Z306 paint diffuse reflectivity with and without addition of microspheres. Improvement with microspheres is constant over the wavelength region. (After Ref. 41.)

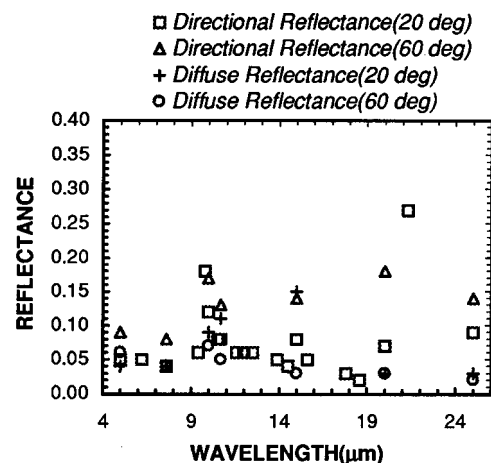


FIG. 21. Sikkens (Akzo) 463 paint directional (specular plus diffuse) and diffuse only reflectance. Significant spectral peaks are seen at 10, 15, and 21 μm . Substrate was raw, stock aluminum.

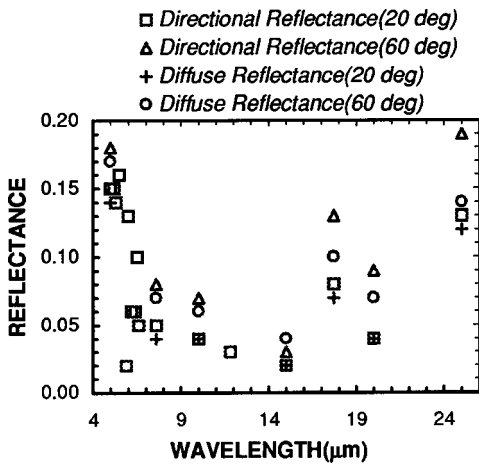


FIG. 22. Eccosorb 268E paint directional (specular plus diffuse) and diffuse only reflectances. Substrate was raw, stock aluminum. Three pronounced features are seen at 5, 17.5, and 25 μm .

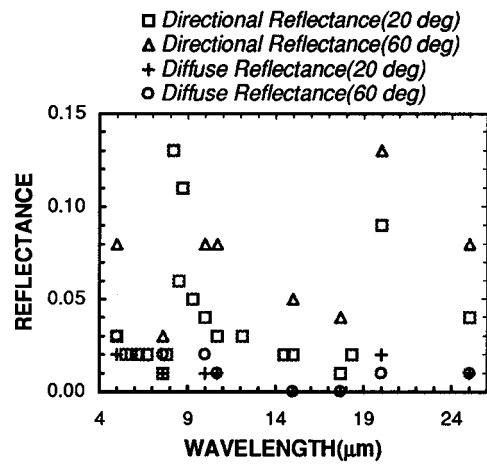


FIG. 24. Teflon directional (specular plus diffuse) and diffuse only reflectances. Sample cut from sheet stock as manufactured. Surface is predominately specular at all wavelengths.

VIII. BIDIRECTIONAL REFLECTANCE DISTRIBUTION FUNCTION (BRDF)

The BRDF is a measure of the diffuse nature of a surface, e.g., providing the extent to which radiation is reflected in different directions from the surface.⁴⁴ In the format used here, a flat profile, indicating a reflectance independent of output angle, illustrates a Lambertian diffuse surface. A sharp peak at a reflection angle corresponding to the incidence angle is typical of specular reflection. For a surface having a total hemispheric reflectance equal to one the maximum value the BRDF can have is $1/\pi$.

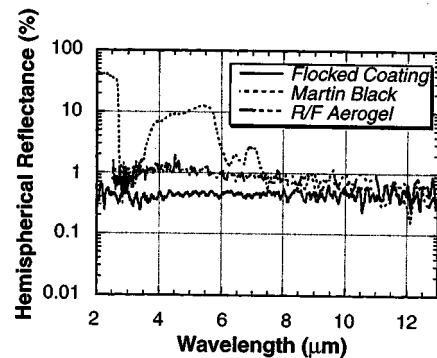


FIG. 25. Spectral reflectance at 8° incident angle for flocked (CLSA96/1) and R/F Aerogel appliqués, compared to Martin Black as known reference. (After Ref. 42.)

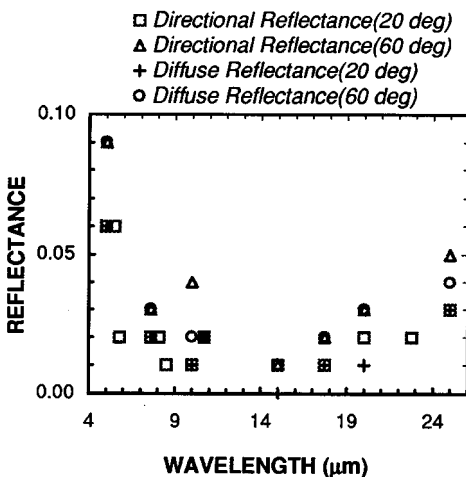


FIG. 23. Parsons Black paint directional (specular plus diffuse) and diffuse only reflectances. Substrate was sandblasted.

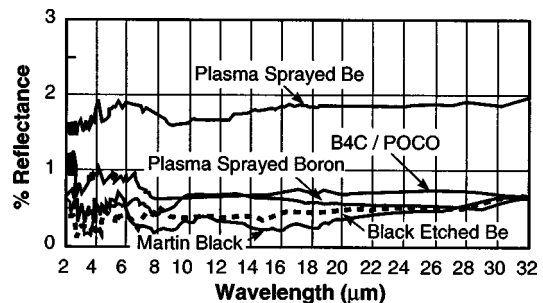


FIG. 26. Spectra of specular reflectance for four diffuse-absorptive baffle surfaces plus Martin Black. (After Ref. 43.)

A. Instrumentation

The five instruments providing BRDF measurements in this review are as follows.

1. Figures 28–30, 37–42, and 47–50

Surface Optics, Corp. using the instrumentation specified in Table VI and illustrated in Fig. 27 took these data for this author.

The instrument is of the goniometer type with parallel beam illumination and detection.⁴⁵ Parallel radiation reflected from the sample is directed by an off-axis parabola to the detector.

The incident angles for these data were $\theta_1 = 20^\circ$, 40° , 60° , and 80° from surface normal in elevation, with $\phi_1 = 0^\circ$ in azimuth. The reflection angles were: in-plane, where $\phi_r = 180^\circ$ is the in-plane forward direction and $\phi_r = 0^\circ$ is the in-plane backward direction; and cross plane, $\phi_r = 90^\circ$ at right angles to in-plane. θ_r is the reflection angle in elevation from surface normal.

Because of the costs associated with these measurements, they were limited to three widely separated wavelengths considered sufficient as a characterization of each surface. In particular, the $10\ \mu\text{m}$ wavelength nearly matches the $10.6\ \mu\text{m}$ commonly used by other experimenters. Filters are used to restrict the source and receiver bandwidths consistent with signal to noise requirements, while not being so wide as to integrate over a large wavelength span.

The BRDF is calibrated by reference to gold plated, sandblasted aluminum. Figures 28 and 29 are BRDFs of highly diffuse and highly specular surfaces provided to illustrate instrument performance.

TABLE VI. Surface Optics Corp. BDR instrumentation used for BRDF measurements.

Type	goniometer with parallel beam illumination and detection
Operation	hemispherical illumination, directional detection directional reflectance by reciprocity
Source bandwidths	$0.1\ \mu\text{m}$ at $5.1\ \mu\text{m}$ $4.44\ \mu\text{m}$ at $9.8\ \mu\text{m}$ $5\ \mu\text{m}$ at $20\ \mu\text{m}$
Source beamwidths	1.1° at $5\ \mu\text{m}$ (black Hardcoat, Teflon, Eccosorb 268E) 2.6° at $5\ \mu\text{m}$ (all others) 2.64° at $9.8, 20\ \mu\text{m}$
Receiver bandwidths	$0.44\ \mu\text{m}$ at $5\ \mu\text{m}$ $0.22\ \mu\text{m}$ at $9.8\ \mu\text{m}$ $0.66\ \mu\text{m}$ at $20\ \mu\text{m}$
Receiver beamwidths	$5\ \mu\text{m}$: 0.44° $10\ \mu\text{m}$: 0.22° $20\ \mu\text{m}$: 0.66°
BRDF noise floor	$5, 10\ \mu\text{m}$: $< 10^{-3}\ \text{ster}^{-1}$ $20\ \mu\text{m}$: $\sim 1/300\ \text{ster}^{-1}$
Angular accuracy	$\pm 0.02^\circ$

2. Figures 31–33, 56, and 57

These measurements were made using the Fully Automated Scatterometer (FASCAT) at Martin Marietta, built by Breault Research Organization.⁴⁶ The instrument was operated at $6328\ \text{\AA}$ and $10.6\ \mu\text{m}$. BRDF is calibrated by comparison with a piece of gold-coated sandpaper having a uniform surface layer of $12\ \mu\text{m}$ grit particles to provide a Lambertian standard. The value is calculated from the measured detector power divided by the detector solid angle, then divided by the product of incident power times the cosine of the incident angle. The abscissa is in units of $\beta - \beta_0 = \sin(\theta_s) - \sin(\theta_i)$, where θ_s is the scatter (reflected) angle and θ_i is the incident angle. $\beta - \beta_0$ approaches zero at the specular angle.

3. Figures 36 and 44–46

These BRDF measurements used the nonspecular reflectometer described in Sec. VII A 4 with the detector at the nonspecular angles. As with the specular reflectance, the BRDF data used a smooth gold-coated surface for calibration, but with the addition of a diffraction correction factor (function of wavelength) necessitated for BRDF in the far infrared.⁴⁷

4. Figure 43

TMA (Bozeman, MT) performed this BRDF measurement. Calibration errors were 2.2% for the near-normal angle, $\theta_i = 5^\circ$.⁴⁸

5. Figures 51 and 52

A modified TMA in-plane scatterometer (CASI model) at the Naval Research Laboratory provides the data in these figures. Note that the BRDF is not cosine corrected.⁴⁹

B. Discussion

1. Martin Black, Infrablack, and Enhanced Martin Black

The Martin Black BRDF in Fig. 30 indicates a wavelength dependence consistent with the spectral reflectance shown previously. The BRDF of $10\text{--}3\ \text{ster}^{-1}$ at $10\ \mu\text{m}$, for incident angles of 30° and 40° and scatter angle of 40° , matches well the value in Fig. 31 by Pompea *et al.* The Lambertian behavior is seen.⁵⁰

Combining Fig. 31 with Figs. 32 and 33 gives a comparison of the three Martin Black types at a common scatter angle and for a common wavelength.⁵¹ They are all fairly similar with nearly Lambertian scattering.

Figures 34 and 35, by Bergener *et al.*, illustrates that Infrablack is slightly superior to Martin Black for near-normal illumination at $10.6\ \mu\text{m}$, but both are Lambertian.

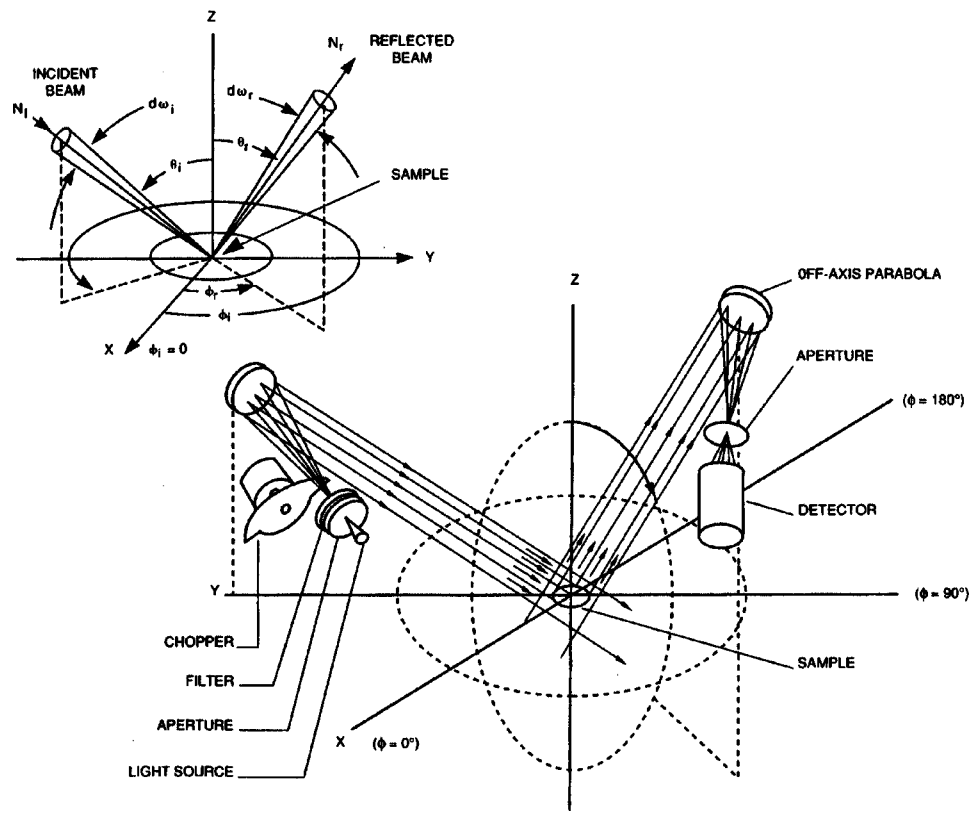


FIG. 27. Surface Optics, Corp. bidirectional reflectometer. Angular definitions and major components are shown. (After Ref. 45.)

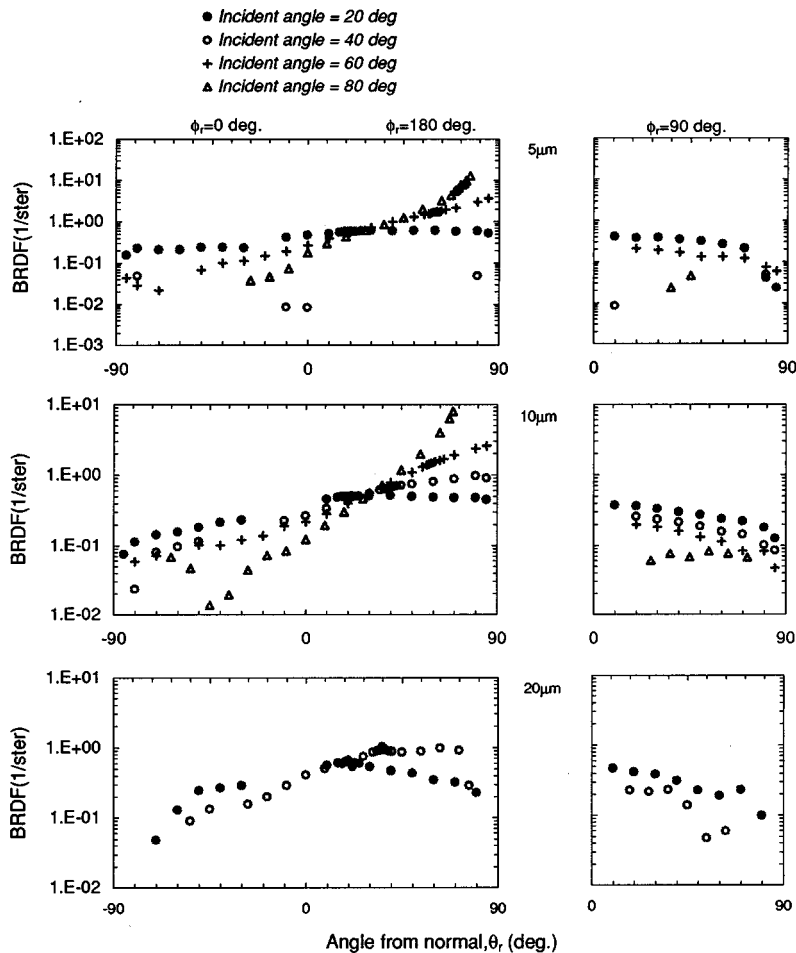


FIG. 28. BRDF of Labsphere, Inc. DSP 200 surface to judge performance of SOC bidirectional reflectometer for a diffuse surface. This is an electrochemical gold plating over sandblasted aluminum substrate ($6 \mu\text{m}$ arithmetic average roughness).

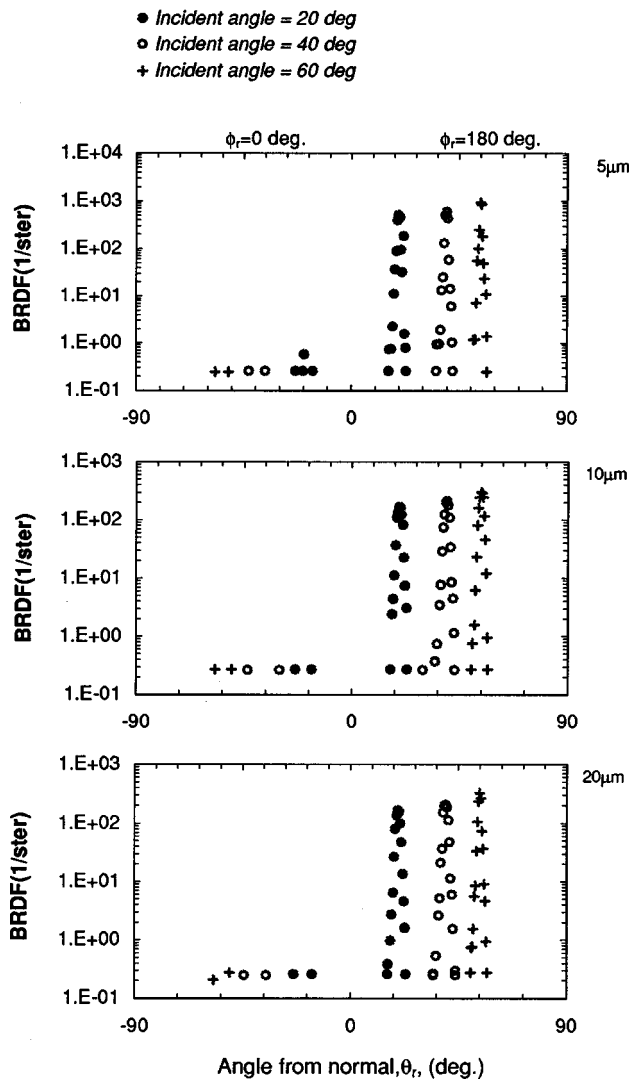


FIG. 29. BRDF of electrolytic gold plating ($10\ \mu\text{m}$ of type III) on nickel-plated and polished aluminum substrate. This provides a calibration of the SOC BRDF instrument's specular response for a specular surface.

However, at 60° from normal Martin Black tends toward specular more than the Infrablack.⁵²

Figure 36, by Smith, is a further comparison of Martin Black with Infrablack, for both long wavelength infrared (LWIR) and far-IR wavelengths. Notable is the increase in specularity at the longer wavelengths. The Infrablack BRDF shows an increase in both the forward and backscatter for glancing reflectance at 12 and $5\ \mu\text{m}$. This result is due to a geometric effect caused by the holes in the Infrablack surface.⁵³

2. Black Anodize, Black Hardcoat, Black Hardlub, and Ebanol C

The effect of surface finish on diffuseness is evidenced by comparison of an anodized sandblasted substrate, Fig. 37, with an anodized polished substrate, Fig. 38. The Hardlub, Fig. 39 and the Hardcoat, Fig. 40, seem very similar considering not only these BRDF but also the spectral reflectances in previous Sec. VII B 2.

Figure 41 indicates that Ebanol C is an extremely diffuse surface, at least at $10\ \mu\text{m}$, and for an incident angle of 20° .

3. Paints

BRDF data for paints are given in Figs. 42–49. Figure 43 by Ames indicates that the desired improvement in BRDF towards a more diffuse version of Chemglaze Z306 is achievable with the addition of microspheres.⁵⁴

Noteworthy is the $12.5\ \mu\text{m}$ BRDF of Ball IR Black (Fig. 44, by Smith). This is a new coating intended to satisfy the requirements of the Space Infrared Telescope Facility (SIRTF) telescope over the broad range of 2–700 μm . The BRDF is Lambertian with values much below the Ames 24E2 that had previously been considered the standard for telescope performance from near IR to far IR. This relative performance is maintained at 66 and 302 μm (see Figs. 45 and 46). It is believed that the low reflectance is due to multiple scatter among the huge surface facets.⁵⁵

4. Teflon

The specularity of Teflon is clearly seen in Fig. 50, consistent with the smooth surface of the sample.

5. Appliqués

Figure 51 is the BRDF of the “biased” appliqué manufactured by ESLI. Recall that the fibers which make up its structure are tilted by 30° – 35° from the normal to the plane of the substrate.⁵⁶ A comparison of a microgrooved appliqué from Battelle with black Kapton appliqué and the conventional Chemglaze Z302 is given in Fig. 52.⁵⁷ Note that the Battelle microstructure leads to different scattering properties depending if the plane of incidence is aligned parallel to or perpendicular to the groove axis. The specular peak is broader for the perpendicular orientation.

6. Advanced optically black surfaces

The BRDFs for a variety of advanced diffuse materials designed for optical baffles are given in Fig. 53.⁵⁸ The profiles are highly Lambertian as required for application as baffled surfaces.

7. Ion beam textured

There is a natural seeding process due to alloyed impurities in blackened 6061-T6 aluminum that results in a broadband texture. This leads to the BRDF in Fig. 54, by Blatchley *et al.* A more homogeneous titanium surface has smaller feature sizes, thus a narrower useful band. The resultant BRDF is given in Fig. 55.⁵⁹

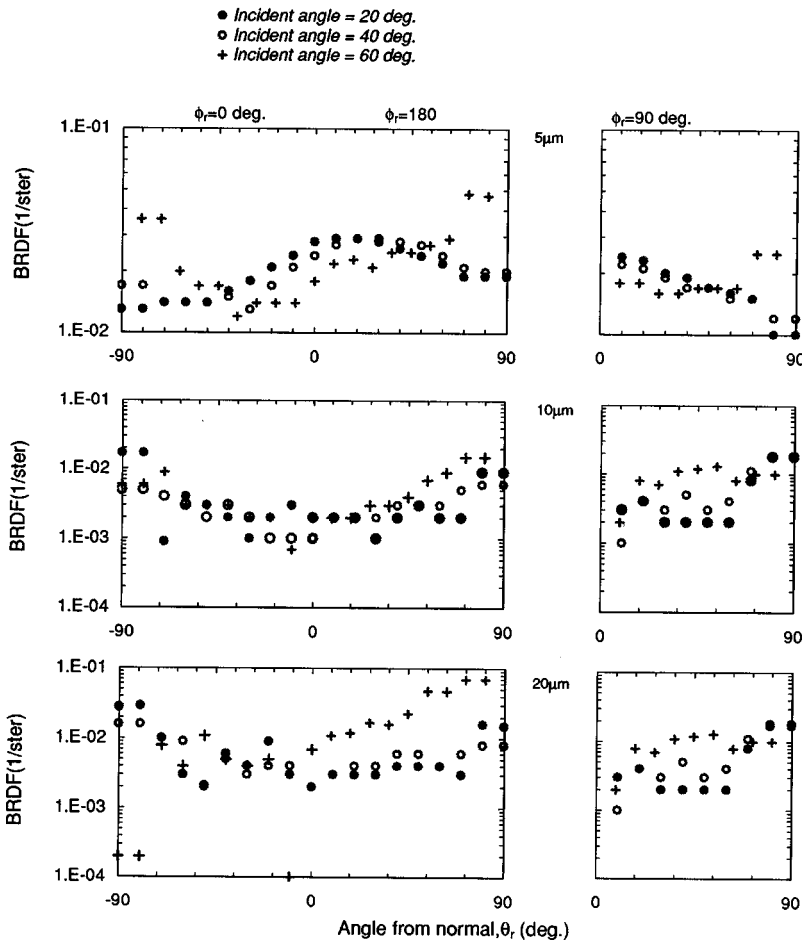


FIG. 30. BRDF of Martin Black. Note the rise at large scatter angles. The BRDF is greatest at 5 μm consistent with the spectral reflectance data.

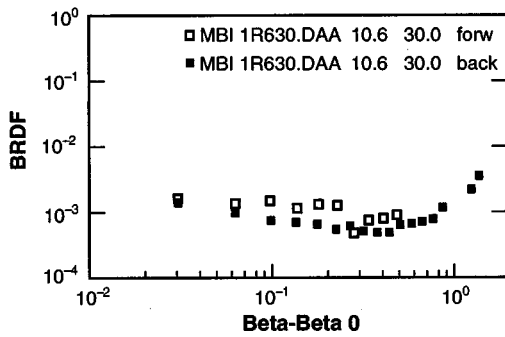


FIG. 31. BRDF of Martin Black using 10.6 μm laser source. Incident angle is 30°. Data are referenced to gold-coated sandpaper (12 μm grit particles) to provide a Lambertian calibration. $\text{Beta} - \text{Beta } 0 = \sin(\theta_s) - \sin(\theta_i)$, where θ_s is the scatter angle and θ_i is the incident angle. (After Ref. 50.)

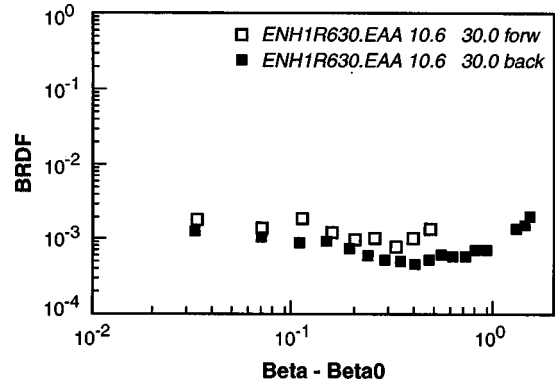


FIG. 33. BRDF of Enhanced Martin Black using 10.6 μm laser source. Incident angle is 30°. (After Ref. 51.)

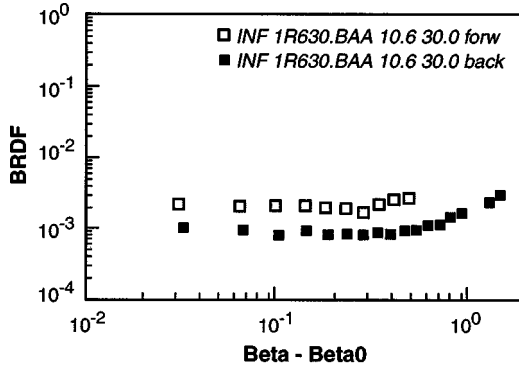


FIG. 32. BRDF of Infrablack using 10.6 μm laser source. Incident angle is 30°. Scatter profile is similar to Martin Black. (After Ref. 51.)

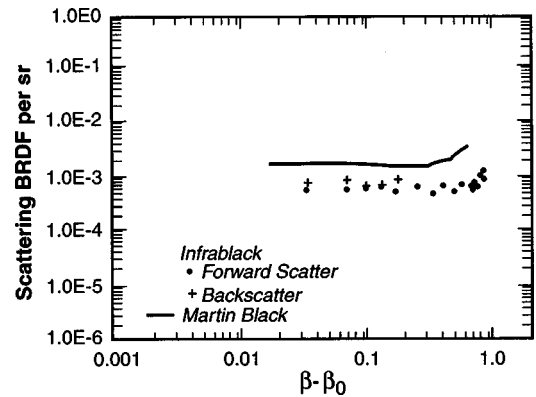


FIG. 34. BRDF of Martin Black and Infrablack at 10.6 μm , for a near normal incident angle of 10°. At this incident angle both surfaces are diffuse. (After Ref. 52.)

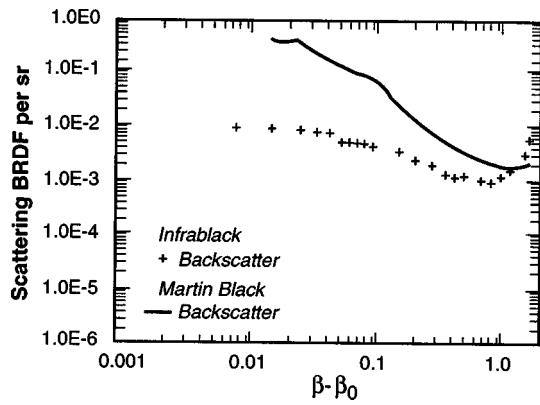


FIG. 35. BRDF of Martin Black and Infrablack at 10.6 μm , for an incident angle of 60° . At this incident angle Martin Black shows specularity. (After Ref. 52.)

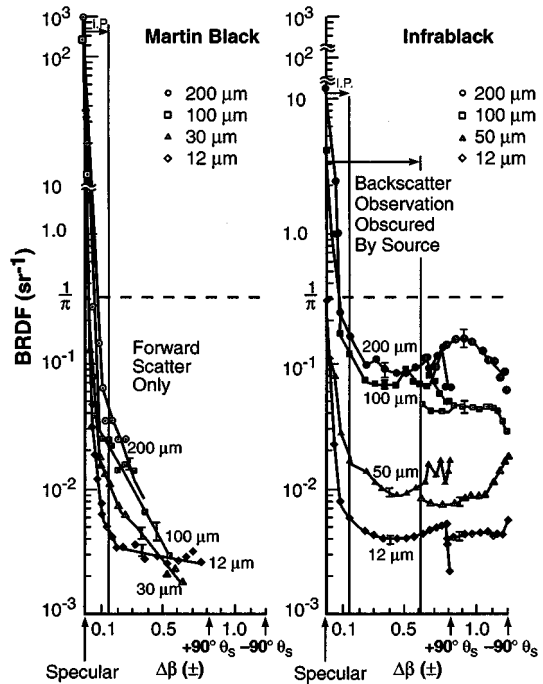


FIG. 36. A comparison of BRDF for Martin Black and Infrablack, as a function of wavelength for an incident angle of 11° . Forward scatter is solid, backscatter is open. Note the statistical error bars. IP is the specular instrument profile. (After Ref. 53.)

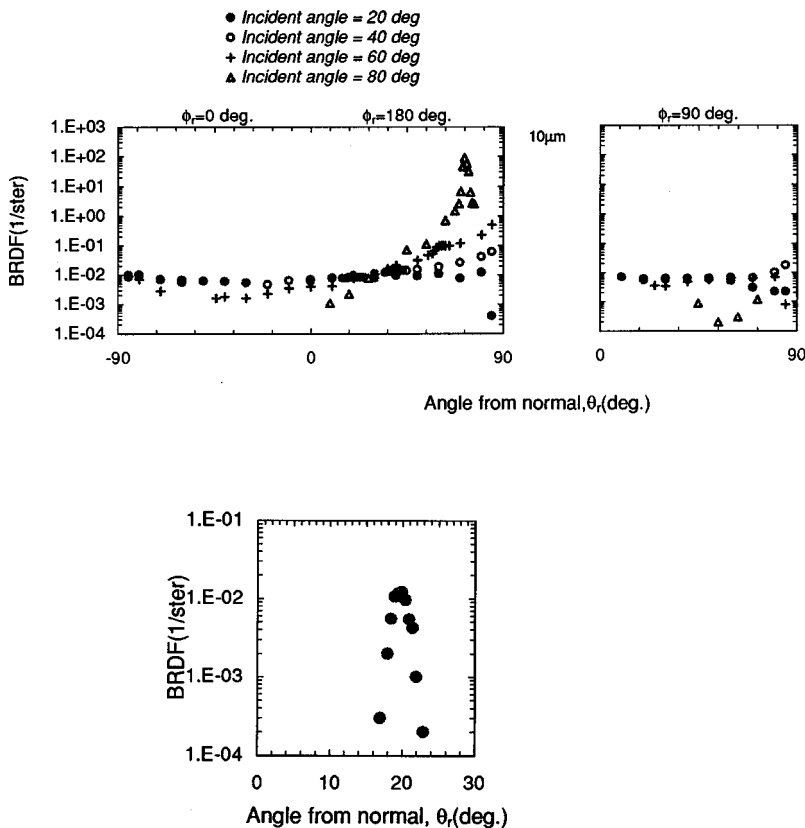


FIG. 37. BRDF for black anodize. Surface was sand-blasted prior to anodization.

FIG. 38. BRDF at 10 μm for black anodize on polished substrate with a 20° incident angle. Reflectance is specular, consistent with a polished substrate.

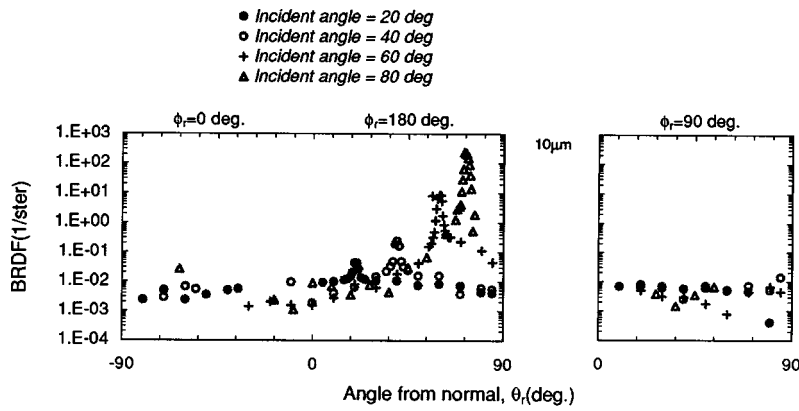


FIG. 39. BRDF for black Hardlub. Surface is specular over a wide range of incident angles. Raw, stock aluminum substrate.

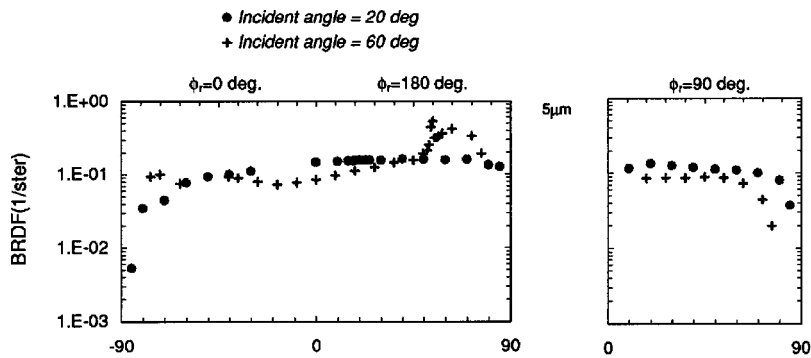


FIG. 40. BRDF for black Hardcoat. The BRDF is particularly specular at 20 μm and 60° incident angle. Sandblasted substrate.

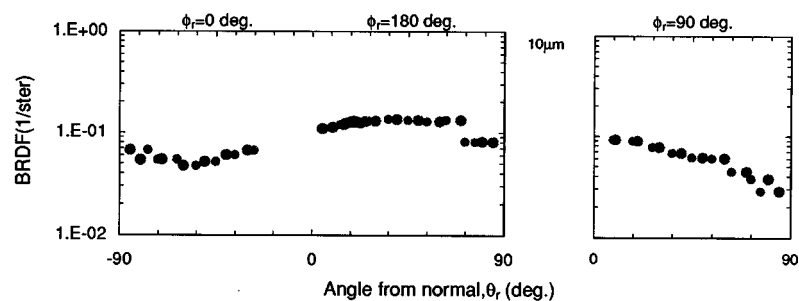
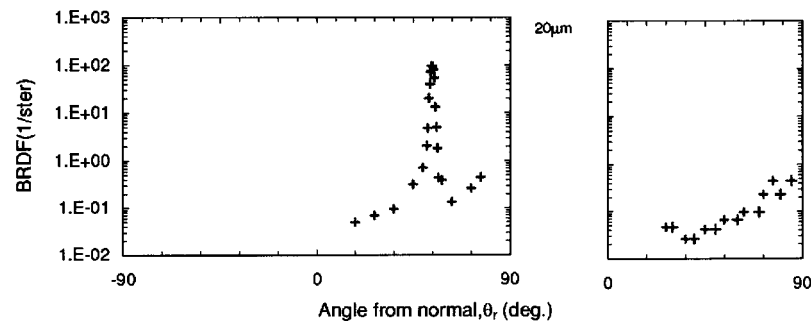
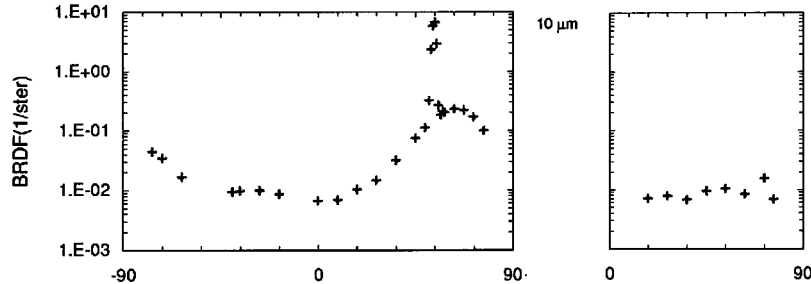


FIG. 41. BRDF for Ebonal C over copper plate on sandblasted substrate. Incident angle is 20°. The BRDF is influenced by diffuse substrate.

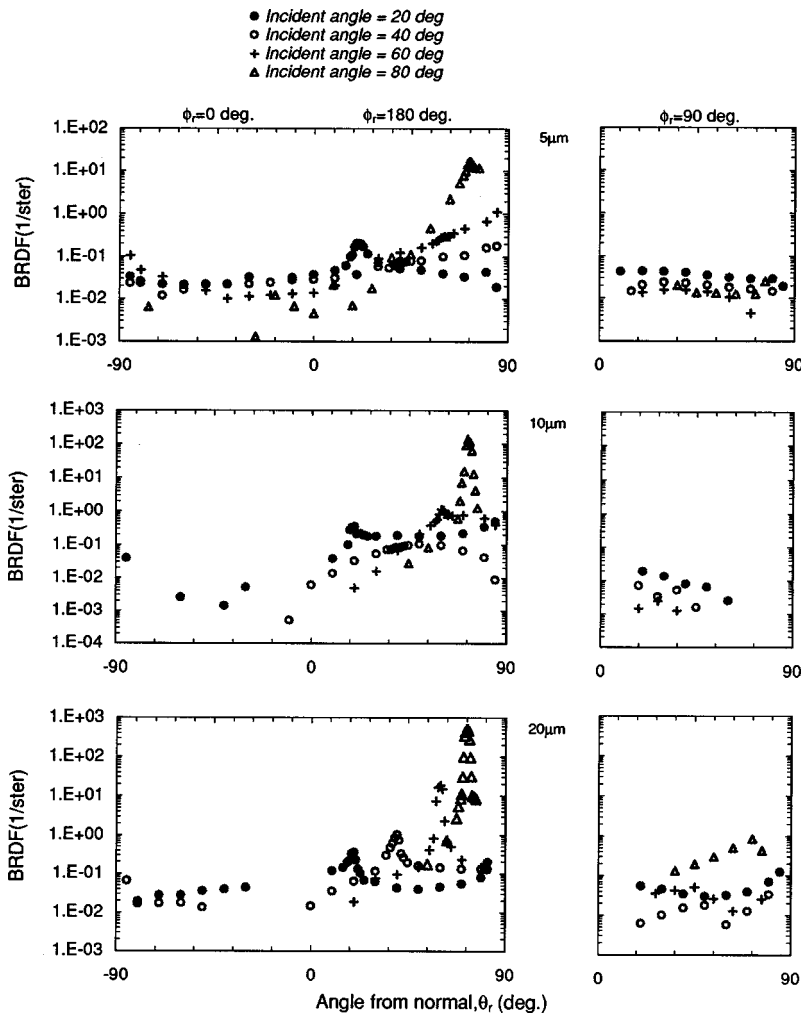


FIG. 42. BRDF for Chemglaze (Aeroglaze) Z306 paint. Specularity increases with wavelength. Substrate was raw stock aluminum.

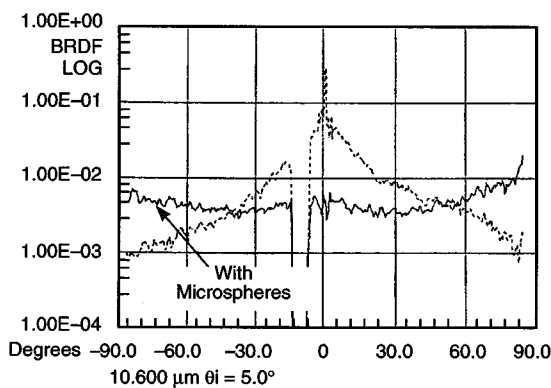


FIG. 43. BRDF for Chemglaze(Aeroglaze) Z306 paint with and without microspheres. The ability of the microspheres to reduce specularity is demonstrated. (After Ref. 54.)

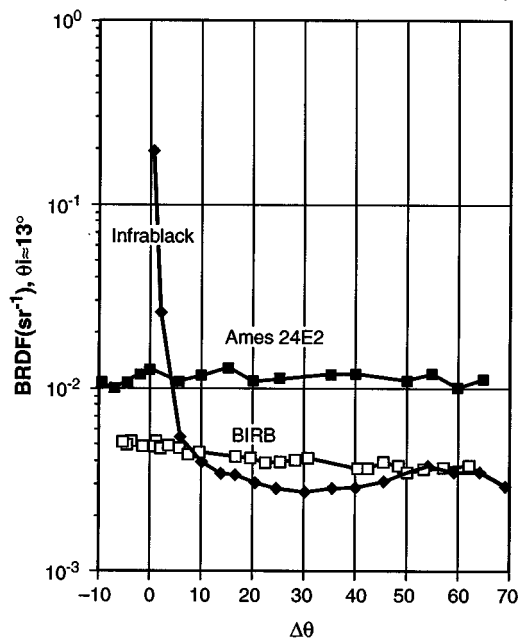


FIG. 44. BRDF of Ball IR Black compared with Infrablack and Ames 24E2 at 12.5 micrometers. Incident angle is 13 degrees. Delta theta is relative to the specular direction. (After Ref. 55.)

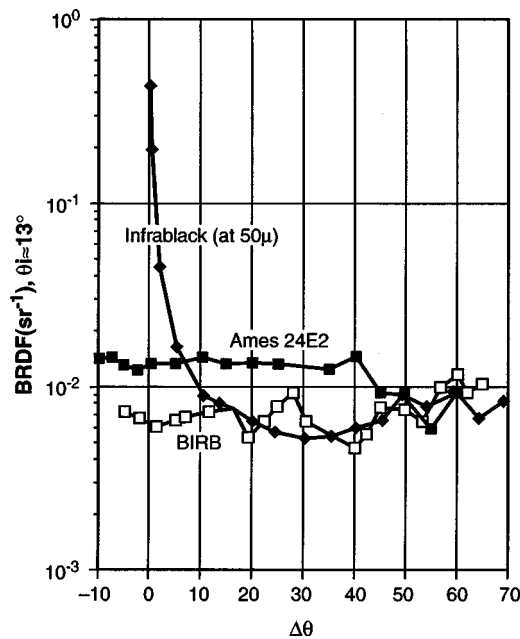


FIG. 45. BRDF of Ball IR Black compared with Infrablack and Ames 24E2. Wavelength is 66 μm except for the Infrablack at 50 μm . Incident angle is 13°. $\Delta\theta$ is relative to the specular direction. (After Ref. 55.)

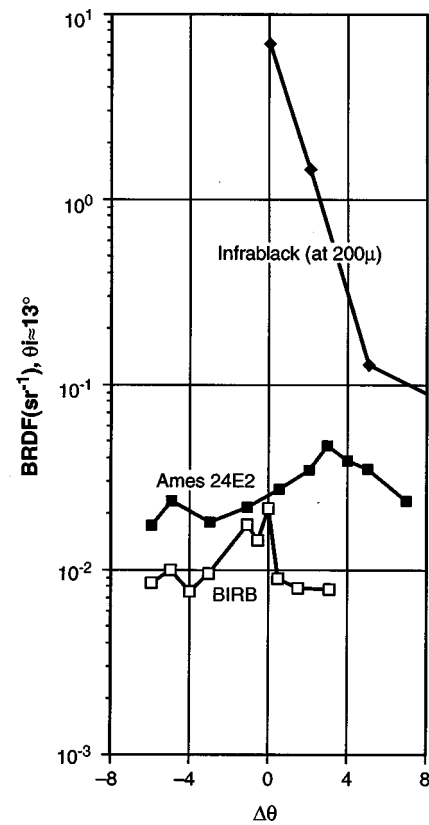


FIG. 46. BRDF of Ball IR Black compared with Infrablack and Ames 24E2. Wavelength is 302 μm except for the Infrablack at 200 μm . Incident angle is 13°. $\Delta\theta$ is relative to the specular direction. (After Ref. 55.)

8. Black chrome

An example of a surface which has a specular BRDF in the infrared but flat BRDF in the visible is given in Figs. 56 and 57, by Pompea *et al.*⁶⁰

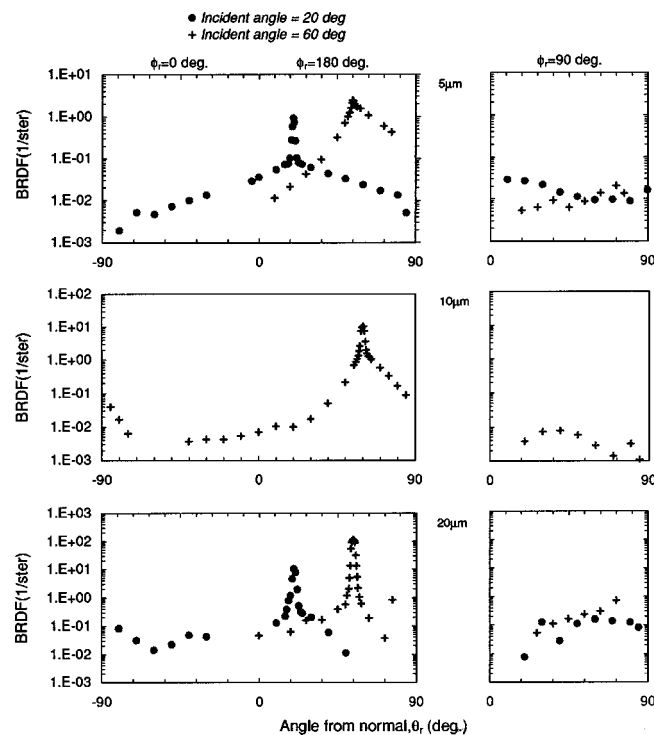


FIG. 47. BRDF of Sikkens(AKZO) 463 paint. BRDF is specular at all three wavelengths measured. Substrate was raw, stock aluminum.

IX. CHEMICAL STABILITY

Surface outgassing and interaction with atomic oxygen are two means by which space-borne surfaces can be degraded.⁶¹ For example, atomic oxygen can affect the binder material in paints. A selection of outgassing data is given in Table VII. Note that variability in paint preparation and test procedures can result in a wide range of results; the values reported here represent the best case, minimum outgassing.

Measurements by Honeywell on the Martin Black indicate an extremely low total weight loss (0.11%) of which less than 0.001% is condensable material.⁶² The use of a dye for visible color seems to have little effect on the outgassing. Note that Ungar gives a Martin Black total material loss of “zero.”⁶³

Tests of the Martin Black on-board the NASA Space

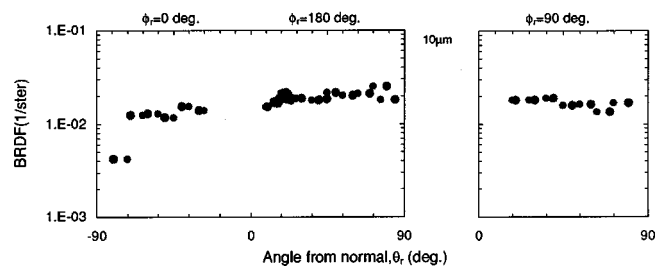


FIG. 48. BRDF of Eccosorb 268E paint. Substrate was raw, stock aluminum.

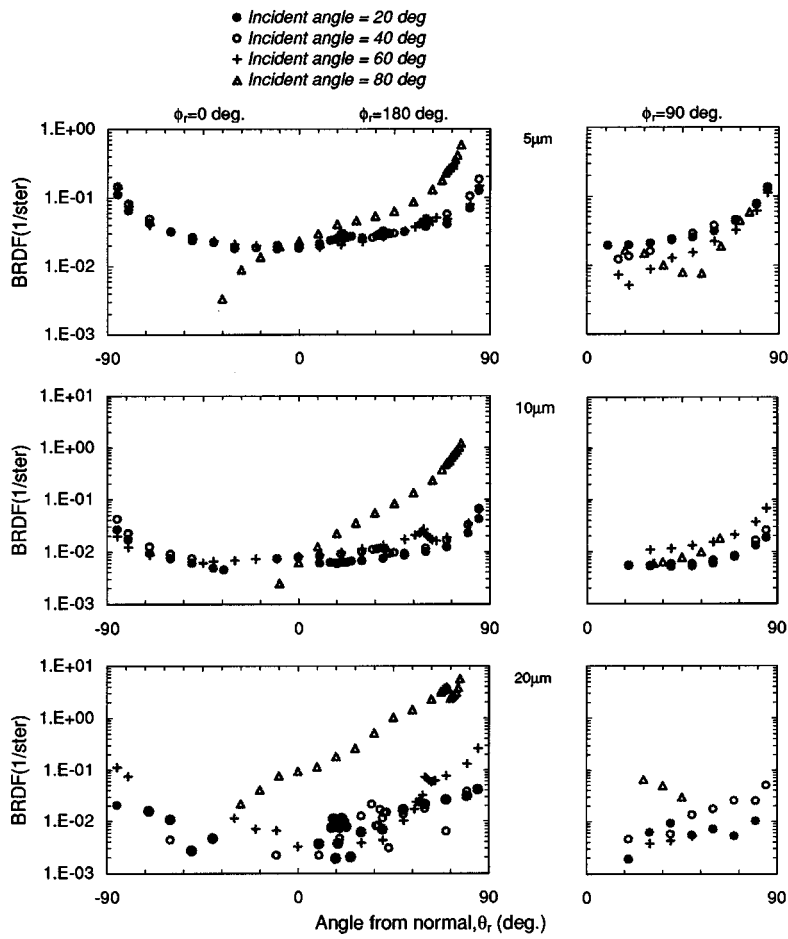


FIG. 49. BRDF of Parsons Black paint on sandblasted substrate.

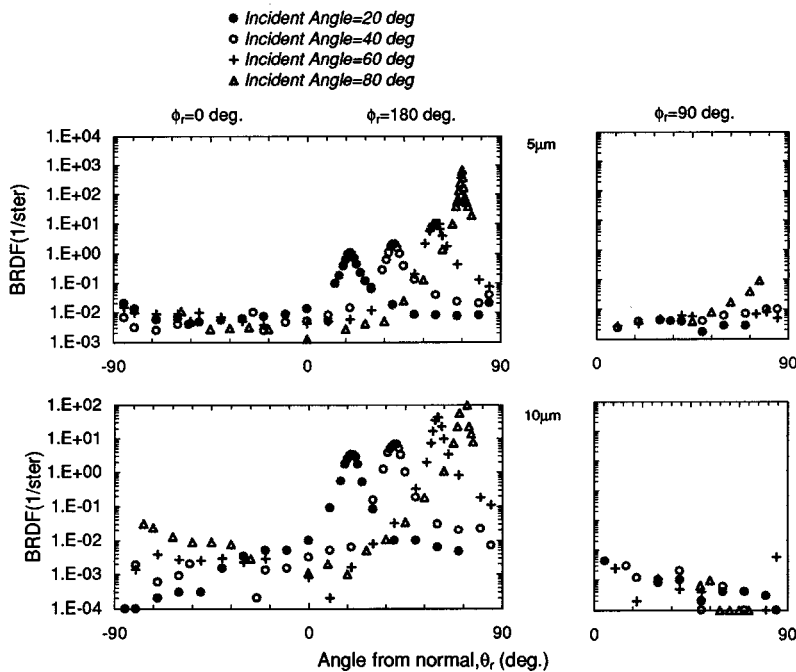


FIG. 50. BRDF of Teflon exhibits significant specularity at both wavelengths measured over a wide range of incident angles. Sample was cut from sheet stock as manufactured.

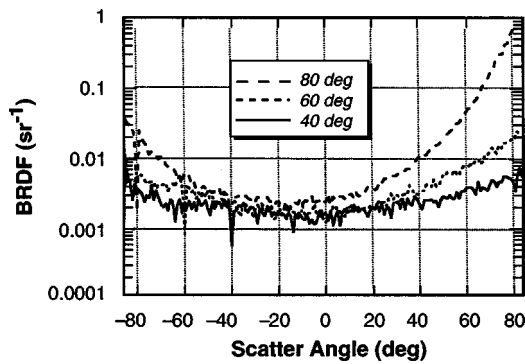


FIG. 51. Biased ESLI surface, in-plane unpolarized BRDF for three incident angles, at 3.39 μm . (After Ref. 56.)

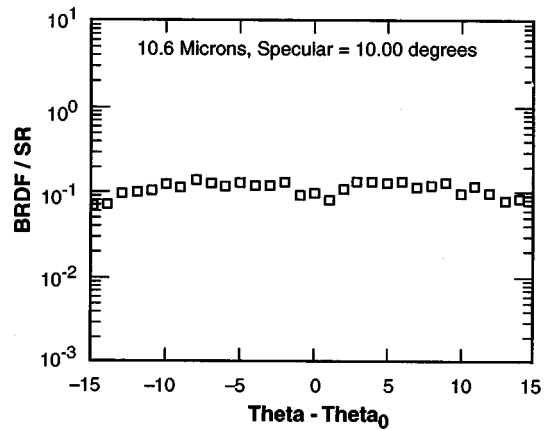


FIG. 54. BRDF for a 6061-T6 aluminum black sample naturally textured to be a broadband surface by the alloy impurities to provide a wide range of feature sizes in surface. Cutoff wavelength is $>25 \mu\text{m}$. (After Ref. 59.)

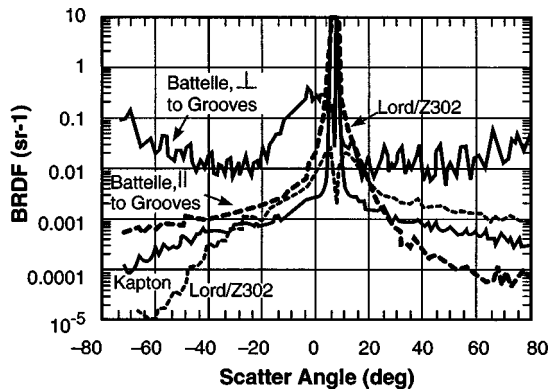


FIG. 52. BRDF of: Battelle microgrooved appliqué, with plane of incidence aligned parallel and perpendicular to the groove axis; and black Kapton appliqué. Data are compared to Lord(Chemglaze) Z302. Incident angle is 7.5° and wavelength is $10.6 \mu\text{m}$. Specular peaks are for Kapton and Lord/Z302. (After Ref. 57.)

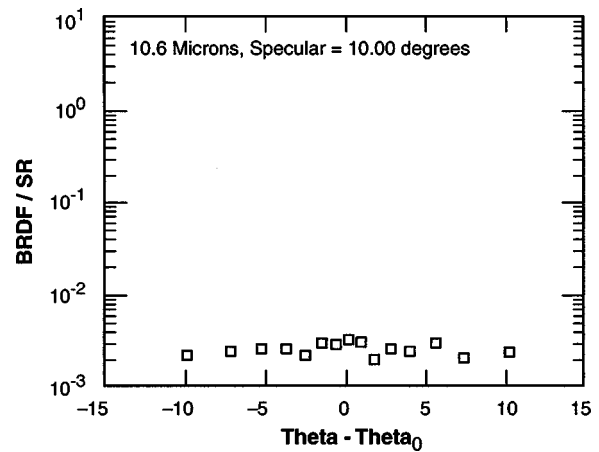


FIG. 55. BRDF for a textured titanium sample. Uniform surface features create a narrow band absorber. (After Ref. 59.)

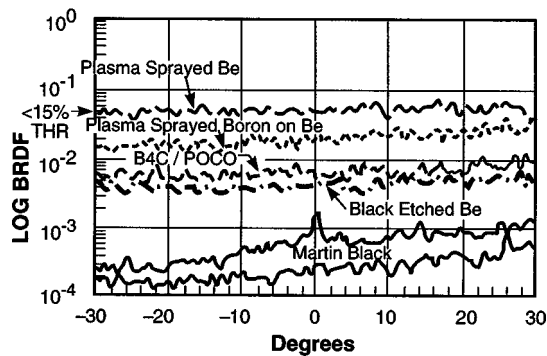


FIG. 53. BRDF of diffuse-absorptive baffle materials and Martin Black at $10.6 \mu\text{m}$. Scatter is Lambertian for each. (After Ref. 58.)

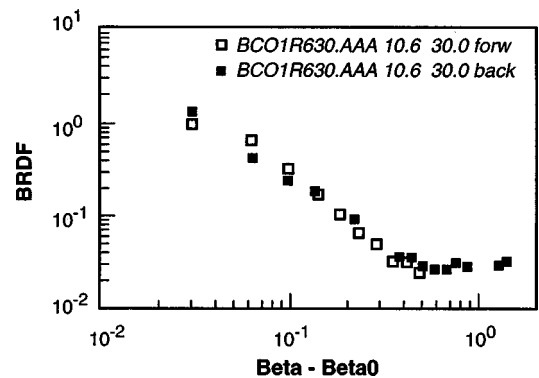


FIG. 56. BRDF at $10.6 \mu\text{m}$ for black chrome. Scattering is specular in the infrared. (After Ref. 60.)

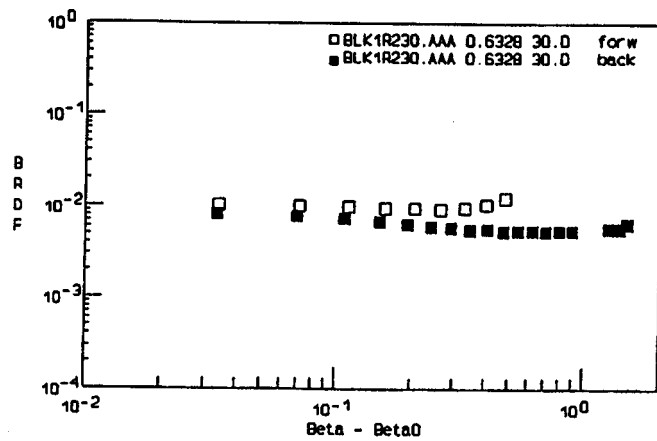


FIG. 57. BRDF at 0.6328 μm for black chrome. Scattering is Lambertian in the visible. (After Ref. 60.)

Shuttle STS-8 addressed erosion due to a ram effect of atomic oxygen streaming past the surface at high velocity, and a possible chemical reaction with the atomic oxygen causing the surface to change its composition. Given a fluence of 3.5×10^{20} atoms/cm² over 41 h exposure the reflectance at 5.6 μm only decreased from 0.32 to 0.24.⁶⁴

X. DISCUSSION

Descriptions and performance data have been provided for a number of black surface treatments.

The data included were obtained for the various authors' applications. Due care should be taken in extrapolating the information to other requirements.

Ideally, optical and mechanical testing for a space-borne sensor component would be of the complete system, e.g., substrate and surface in the configuration of actual use. Usually this is not possible and witness samples of the surface treatments were substituted for the purpose of these data. The configurations were based on the available instrumentation described here. For purposes other than these, consideration must be given early in the design phase to the test instrumen-

TABLE VII. Black surface material outgassing.

Test conditions: after 24 h@125C in vacuum per ASTM E595-77/84/90 except Martin Black per NASA-SP-R-0022. Cure temperature=25C; cure atmosphere=air. (Reference 87.)

Surface	TML ^a (%)	CVCM ^b (%)	WVR ^c (%)	Cure time
AMES 24E	0.67	0.16	0.07	7D
Black anodize	0.75	0.02		
Chemglaze Z306	2.31	0.02	0.82	16H
CTL-15	2.16	0.06	0.35	30M
Eccosorb CR-110	0.52	0.00	0.19	16H
Martin Black	0.11	negligible		
MSA 94B	3.66	0.00	3.59	16H
Sikkens 463	4.05	0.03		1H
Parsons Black	13.33	3.65		

^aTML: Total mass loss.

^bCVCM: Collected volatile condensable materials.

^cWVR: Water vapor retained (in 24 hours while exposed to 25C, 50% relative humidity).

tation and to the design of the test samples to best reflect the actual use.

Finally, it is important that the selection for a given application take into consideration the overall system design, not just these properties of the surface taken alone. The surface treatment need not be the first consideration but it must not be the last.

ACKNOWLEDGMENTS

The Ballistic Missile Defense Organization/AQS, under Air Force Contract No. F19628-90-C-0002 sponsored the author's measurements. Significant contributions were provided by Dr. Douglas Cohen, Leonard Gordan, and Dr. Perry Longaker of MIT/Lincoln Laboratory; Fred Davino of Plating for Electronics; and Dr. J. T. Neu of Surface Optics, Corp. The author is particularly indebted to all those who provided personal communications as listed in the references, and especially, Dr. Susan McCall of Soric, Inc.

¹I use ...ance to refer to measurements of actual surfaces and ...ivity to refer to intrinsic properties as suggested in the *Handbook of Optics*, Volume II, (McGraw-Hill, New York, 1995), p. 25.3.

²Additional information on surface treatments and design issues is presented in *Handbook of Optics*, Volume II, Black Surfaces for Optical Systems, edited by S. M. Pompea and R. P. Breault, M. Bass, Editor in Chief (McGraw-Hill, New York, 1995), Chap. 37; S. M. Pompea and S. H. C. P. McCall, Proc. SPIE **1753**, (1992). Databases of surface properties are discussed in S. H. C. P. McCall, S. M. Pompea, R. P. Breault, and N. L. Regens, Proc. SPIE **1753**, 158 (1992); S. H. C. P. McCall, R. P. Breault, A. E. Piotrowski, J. W. Rodney, and L. A. Piotrowski, Proc. SPIE **2864**, 308 (1996); S. H. C. P. McCall, L. B. Begrambekov, and J. Elder Pierre, Proc. SPIE **2260**, 178 (1994).

³G. L. Peterson and S. C. Johnston, Proc. SPIE **1753**, 65 (1992).

⁴R. D. Seals and M. B. McIntosh, Proc. SPIE **1753**, 196 (1992).

⁵T. G. Hawarden, R. Crane, H. A. Thronson, A. J. Penny, A. H. Orlowska, and T. W. Bradshaw, Space Sci. Rev. **74**, 45 (1995).

⁶E. M. Wooldridge, NASA/Goddard Space Flight Center, Proc. 7th International Symposium on Materials in Space Environment, SP-399, 1997 (unpublished), p. 127.

⁷A. Thurgood, Proceedings of the BMD Metrology Program Review, 17 & 18 December 1996, National Institute of Standards and Technology, Gaithersburg, Maryland (unpublished).

⁸C. Hamilton, J. Howard, and T. Murdock, Proceedings of the Seventh SDL/USU and NIST Symposium on Infrared Radiometric Sensor Calibration, Utah State University, Logan, Utah, (1997).

⁹A. J. Ames, Proc. SPIE **1331**, 300 (1990).

¹⁰S. M. Pompea and R. P. Breault, p37.17.

¹¹D. Shepard [donald.f.shepard@lmco.com] (personal communication).

¹²S. M. Smith, Proc. SPIE **967**, 249 (1988).

¹³S. M. Pompea, D. W. Bergener, D. F. Shepard, and S. Russak, Opt. Eng. (Bellingham) **23**, 151 (1984).

¹⁴S. M. Smith, Proc. SPIE **2260**, 206 (1994).

¹⁵S. M. Pompea, D. F. Shepard, and S. Anderson, Proc. SPIE **967**, 237 (1988).

¹⁶S. M. Smith, Proc. SPIE **967**, 249 (1988).

¹⁷W. M. Bloomquist and D. F. Shepard, Proc. SPIE **2864**, 368 (1996).

¹⁸S. M. Smith, Proc. SPIE **967**, 249 (1988).

¹⁹S. M. Smith and J. C. Fleming, Proc. SPIE **3426**, (1998).

²⁰K. Snail, D. P. Brown, J. Costantino, W. C. Shemano, C. W. Schmidt, W. F. Lynn, C. L. Seaman, and T. R. Knowles, Proc. SPIE **2864**, 465 (1996).

²¹K. Snail [Snail@NRL.NAVY.MIL] (personal communication).

²²C. C. Blatchley, E. A. Johnson, Y. Kang Pu, and C. Von Benken, Proc. SPIE **1753**, 317 (1992).

²³S. M. Pompea, D. F. Shepard, and S. Anderson, Proc. SPIE **967**, 238 (1988).

²⁴R. D. Seals and M. B. McIntosh, Proc. SPIE **1753**, 196 (1992).

²⁵Y. Kameda [kameda@uchu.komukai.toshiba.co.jp] (personal communication).

- ²⁶E. Ramberg [eramberg@ball.com] (personal communication).
- ²⁷L. Kauder, NASA Space Flight Center (personal communication).
- ²⁸S. H. C. P. McCall [mccall@soric.com] (personal communication).
- ²⁹J. J. Bock, Ph.D. thesis, University of California at Berkeley, 1994.
- ³⁰T. R. Sampair and W. M. Berrios, NASA Langley Research Center, Hampton, VA, NASA-CP-3134, pp. 935–944 (1992).
- ³¹C. F. Wilson, *Proc. Fourth SDL/USU Symposium on Infrared Radiometric Sensor Calibration*, Space Dynamics Laboratory, Utah State University, Logan, Utah (1994).
- ³²M. T. Beecroft (personal communication); for additional information see also: M. T. Beecroft, J. T. Neu, and J. Jafolla, *Proc. SPIE* **1753**, 304 (1992).
- ³³A. L. Shumway, D. F. Shepard, R. E. Clement and P. McKenna, *Proc. SPIE* **2864**, 387 (1996).
- ³⁴A. L. Shumway, D. F. Shepard, R. E. Clement, and P. McKenna, *Proc. SPIE* **2864**, 389 (1996).
- ³⁵S. M. Smith, *Proc. SPIE* **967**, 248 (1988).
- ³⁶A. J. Ames, *Proc. SPIE* **1331**, 300 (1990).
- ³⁷S. M. Smith, *Proc. SPIE* **2260**, 204 (1994).
- ³⁸A. L. Shumway *et al.*, *Proc. SPIE* **2864**, 391 (1996).
- ³⁹A. L. Shumway, D. F. Shepard, R. E. Clement, and P. McKenna, see Ref. 38, p. 392.
- ⁴⁰S. M. Smith, *Proc. SPIE* **967**, 250 (1988).
- ⁴¹A. J. Ames, *Proc. SPIE* **1331**, 301 (1990).
- ⁴²K. Snail (personal communication).
- ⁴³R. D. Seals and M. B. McIntosh, *Proc. SPIE* **1753**, 199 (1992).
- ⁴⁴The concept of BRDF is presented in: F. E. Nicodemus, J. C. Richmond, J. J. Hsia, I. W. Ginsberg, and T. Limperis, U.S. Department of Commerce, National Bureau of Standards, Washington, D.C 20234, (1977).
- ⁴⁵M. T. Beecroft, *Proc. SPIE* **1753**, 307 (1992).
- ⁴⁶S. M. Pompea, *Proc. SPIE* **967**, 237 (1988).
- ⁴⁷S. M. Smith, *Proc. SPIE* **967**, 251 (1988).
- ⁴⁸A. J. Ames, *Proc. SPIE* **1331**, 301 (1990).
- ⁴⁹K. Snail, D. P. Brown, J. Costantino, W. C. Shemano, C. W. Schmidt, W. F. Lynn, C. L. Seaman, and T. R. Knowles, *Proc. SPIE* **2864**, 466 (1996).
- ⁵⁰S. M. Pompea, D. F. Shepard, and S. Anderson, *Proc. SPIE* **967**, 240 (1988).
- ⁵¹S. M. Pompea, D. F. Shepard, and S. Anderson, see Ref. 50, pp. 241 and 242.
- ⁵²D. W. Bergener, S. M. Pompea, and D. F. Shepard, *Proc. SPIE* **511**, 67 (1984).
- ⁵³S. M. Smith, *Proc. SPIE* **967**, 252 (1988).
- ⁵⁴A. J. Ames, *Proc. SPIE* **1331**, 304 (1990).
- ⁵⁵S. M. Smith and J. C. Fleming, *Proc. SPIE* **3426**, (1998).
- ⁵⁶K. Snail, D. P. Brown, J. Costantino, W. C. Shemano, C. W. Schmidt, W. F. Lynn, C. L. Seaman, and T. R. Knowles, *Proc. SPIE* **2864**, 471 (1996).
- ⁵⁷K. Snail, D. P. Brown, J. Costantino, W. C. Shemano, C. W. Schmidt, W. F. Lynn, C. L. Seaman, and T. R. Knowles, *Proc. SPIE* **2864**, 470 (1996).
- ⁵⁸R. D. Seals and M. B. McIntosh, *Proc. SPIE* **1753**, 199 (1992).
- ⁵⁹C. C. Blatchley, E. A. Johnson, Y. K. Pu, and C. Von Benken, *Proc. SPIE* **1753**, 324 (1992).
- ⁶⁰S. M. Pompea, D. F. Shepard, and S. Anderson, *Proc. SPIE* **967**, 245 (1988).
- ⁶¹See also: S. H. C. P. McCall, *et al.*, *Proc. SPIE* **2260**, 33 (1994); J. S. Dyer, R. C. Benson, and J. J. Guregian, *Proc. SPIE* **1754**, 177 (1992); D. M. Silver, R. C. Benson, J. W. Garrett, and A. P. M. Glassford, *Proc. SPIE* **2261**, 160 (1994); C. M. Egart and J. A. Basford, *Proc. SPIE* **1330**, 178 (1990).
- ⁶²D. F. Shepard [donald.f.shepard@lmco.com] (personal communication).
- ⁶³S. Ungar, J. Mangin, M. Lutz, G. Jeandel, and B. Wyncke *Proc. SPIE* **1157**, 375 (1989).
- ⁶⁴S. M. Pompea, D. W. Bergener, D. F. Shepard, and K. S. Williams, *Proc. SPIE* **511**, 27 (1984).
- ⁶⁵S. M. Pompea, D. W. Bergener, D. F. Shepard, S. Russak, and W. L. Wolfe, *Opt. Eng.* **23**, 149 (1984).
- ⁶⁶S. M. Pompea, D. F. Shepard, and S. Anderson, *Proc. SPIE* **967**, 236 (1988).
- ⁶⁷S. H. C. P. McCall [mccall@soric.com] (personal communication).
- ⁶⁸J. Young [jyoung@west.raytheon.com] (personal communication).
- ⁶⁹M. Endemann [mendeman@estec.esa.nl] (personal communication).
- ⁷⁰I. M. Mason, P. H. Sheather, J. A. Bowles, and G. Davies, *Appl. Opt.* **35**, 629 (1996).
- ⁷¹J. F. Kordas, H.-S. Park, I. T. Lewis, B. A. Wilson, R. E. Priest, M. J. Shannon, W. T. White III, A. G. Ledebuhr, D. P. Nielsen, and L. D. Pleasance, *Proc. SPIE* **2478**, 179 (1995).
- ⁷²J. F. Kordas, R. E. Priest, I. T. Lewis, R. F. Hills, B. A. Wilson, M. J. Shannon, D. P. Nielsen, A. G. Ledebuhr, H.-S. Park, and L. D. Pleasance, *Proc. SPIE* **2466**, 75 (1995).
- ⁷³J. S. Dyer, R. C. Benson, T. E. Phillips, and J. J. Guregian, *Proc. SPIE* **1754**, 177 (1992).
- ⁷⁴D. Lencioni [MIT Lincoln Laboratory] (personal communication).
- ⁷⁵B. Saggin [saggin@dim.unipd.it] (personal communication).
- ⁷⁶D. Eckert [dbeckert@itt.com] (personal communication).
- ⁷⁷D. F. Everett [deverett@sunland.gsfc.nasa.gov] (personal communication).
- ⁷⁸S. H. C. P. McCall [mccall@soric.com] (personal communication).
- ⁷⁹R. E. Priest, H.-S. Park, L. D. Pleasance, I. T. Lewis, M. J. Shannon, M. A. Massie, N. R. Sewall, A. G. Ledebuhr, and K. Metschuleit, *Proc. SPIE* **2475**, 408 (1995).
- ⁸⁰R. E. Priest, H.-S. Park, L. D. Pleasance, I. T. Lewis, M. J. Shannon, M. A. Massie, N. R. Sewall, A. G. Ledebuhr, and K. Metschuleit, *Proc. SPIE* **2475**, 396 (1995).
- ⁸¹C. L. Mosier [Carol.L.Mosier.1@gsfc.nasa.gov] (personal communication).
- ⁸²Y. Kameda [kameda@uchu.komukai.toshiba.co.jp] (personal communication).
- ⁸³E. Ramberg [eramberg@ball.com] (personal communication).
- ⁸⁴J. J. Bock [jjb@astro.caltech.edu] (personal communication).
- ⁸⁵T. D. Wise, *Proc. SPIE* **2864**, 364 (1996).
- ⁸⁶J. H. Henninger, *Solar Absorptance and Thermal Emittance of Some Common Spacecraft Thermal-Control Coatings* (NASA Reference Publication 1121, Goddard Space Flight Center, Greenbelt, MD, 1984), p. 7.
- ⁸⁷D. Shepard [donald.f.shepard@lmco.com] (personal communication) all others: W. A. Campbell, Jr. and J. J. Scialone, *Outgassing Data for Selecting Spacecraft Materials* (NASA Reference Publication 1124, Rev. 3, Goddard Space Flight Center, Greenbelt, MD, 1993).